

AD-A009 438

INVESTIGATION OF ELECTRONIC TRANSPORT,
RECOMBINATION AND OPTICAL PROPERTIES
IN $\text{InAs}_{1-x}\text{P}_x$ ALLOY SYSTEMS

Sheng S. Li

Florida University

Prepared for:

Army Electronics Command
Advanced Research Projects Agency

15 December 1974

DISTRIBUTED BY:

NTIS

National Technical Information Service
U. S. DEPARTMENT OF COMMERCE

ADA009438

140073

INVESTIGATION OF ELECTRONIC TRANSPORT,
RECOMBINATION AND OPTICAL PROPERTIES
IN $\text{InAs}_{1-x}\text{P}_x$ ALLOY SYSTEMS

SECOND SEMI-ANNUAL TECHNICAL REPORT
(June-November, 1974)

By

Sheng S. Li
Tel. (904) 392-4927

December 15, 1974



NIGHT VISION LABORATORY
U.S. ARMY ELECTRONICS COMMAND
FORT BELVOIR, VIRGINIA 22060

SPONSORED BY
ADVANCED RESEARCH PROJECTS AGENCY
ARPA ORDER 2182
PROGRAM CODE 4D10
CONTRACT DAAK02-74-C-0102

Effective Date: December 1, 1973
Expiration: November 30, 1975

Electrical Engineering Department
College of Engineering
University of Florida
Gainesville, Florida 32611



The views and conclusion contained in this document are those of the authors and should not be interpreted as necessarily representing the official policies, either expressed or implied, of the Defense Advanced Research Projects Agency of the U.S. Government.

Distribution Statement

Approved for public release;
distribution unlimited.

Reproduced by
NATIONAL TECHNICAL
INFORMATION SERVICE
U.S. Department of Commerce
Springfield, VA. 22151

REPORT DOCUMENTATION PAGE		READ INSTRUCTIONS BEFORE COMPLETING FORM
1. REPORT NUMBER Progress Report No. 2	2. GOVT ACCESSION NO.	3. RECIPIENT'S CATALOG NUMBER
4. TITLE (and Subtitle) Investigation of Electronic Transport, Recombination and Optical Properties in InAs _{1-x} P _x Alloy Systems		5. TYPE OF REPORT & PERIOD COVERED 2nd Semi-Annual Technical; June-December 1974
		6. PERFORMING ORG. REPORT NUMBER
7. AUTHOR(s) Sheng S. Li		8. CONTRACT OR GRANT NUMBER(s) DAAK02-74-C-0102
9. PERFORMING ORGANIZATION NAME AND ADDRESS University of Florida Engineering & Industrial Experiment Station Gainesville, Florida 32611		10. PROGRAM ELEMENT, PROJECT, TASK AREA & WORK UNIT NUMBERS 2182, n/a, n/a 4D10 DOD supplement
11. CONTROLLING OFFICE NAME AND ADDRESS		12. REPORT DATE December 15, 1974
14. MONITORING AGENCY NAME & ADDRESS (if different from Controlling Office) Night Vision Laboratory U.S. Army Electronics Command Fort Belvoir, Virginia 22060		13. NUMBER OF PAGES 63
		15. SECURITY CLASS. (of this report) unclassified
		15a. DECLASSIFICATION/DOWNGRADING SCHEDULE
16. DISTRIBUTION STATEMENT (of this Report) Approved for public release; distribution unlimited.		
17. DISTRIBUTION STATEMENT (of the abstract entered in Block 20, if different from Report)		
18. SUPPLEMENTARY NOTES This research was supported by the Defense Advanced Research Project Agency.		
19. KEY WORDS (Continue on reverse side if necessary and identify by block number) InAs _{1-x} P _x epitaxial samples, electrical resistivity, Hall coefficient, electron mobility, electron concentration, magnetoresistance coefficient, optical absorption coefficient, energy band gap.		
20. ABSTRACT (Continue on reverse side if necessary and identify by block number) A systematic study has been carried out on the dependence of the electron mobility and concentration on the epitaxial layer thickness for seven InAs _{0.65} P _{0.35} epitaxial samples (164-171) with film thickness varying from 10μm to 4μm. (It was found that an epilayer thickness around 6μm yields the highest electron mobility and lowest electron concentration for this set of samples (i.e., μ=13500 cm ² /V-S and n=8.5x10 ¹⁵ cm ⁻³ at 77°K.) A technique has been developed in our Laboratory to examine the atomic composition, the		

DD FORM 1473

1 JAN 73

EDITION OF 1 NOV 65 IS OBSOLETE
S/N 0102-014-6601PRICES SUBJECT TO CHANGE
unclassified

SECURITY CLASSIFICATION OF THIS PAGE (When Data Entered)

20. (cont'd.) epilayer thickness and the homogeneity of the epilayer using Electron Microprobe Analysis. The optical absorption coefficient as a function of wavelength near the fundamental absorption edge was plotted for 13 epitaxial samples (147-159) of different alloy compositions. The energy band gap versus alloy composition for these samples was also determined.

ia

unclassified

SECURITY CLASSIFICATION OF THIS PAGE(When Data Entered)

FOREWORD

This technical report covers the research activities between June and December 1974 under contract DAAK02-74-C-0102. Mr. David Jackson, Jr., (AMSEL-NV-II) is the responsible Army Night Vision Contract monitor. This work was executed by the Department of Electrical Engineering of the University of Florida, Gainesville, Florida. The principal investigator of this research project is Dr. Sheng S. Li. Major contributors are J. R. Anderson, D. W. Schoenfeld and R. A. Owen. Additional support was derived during this reporting period from Dr. J. K. Kennedy of the Air Force Cambridge Research Laboratory, who so generously prepared the necessary $\text{InAs}_{1-x}\text{P}_x$ epitaxial films for this contract research.

ABSTRACT

The research program sponsored by this contract during the past six months period has produced technical findings in several areas: (1) A technique has been developed in our Laboratory enabling us to examine simultaneously the atomic compositions, the epi-layer thickness and the homogeneity of the film across both the GaAs substrate and the InAsP epilayer using Electron Microprobe analysis. (2) A systematic study has been carried out on the correlations between the electron mobility and epilayer thickness and between the electron concentration and the epilayer thickness for six InAsP epitaxial samples. (3) The resistivity and the Hall coefficient data yielded electron mobility and electron concentration for samples 164 to 171; the highest electron mobility observed was $13500 \text{ cm}^2/\text{V-S}$ at 77°K , and the lowest electron density observed was $8.5 \times 10^{15} \text{ cm}^{-3}$ also at 77°K . (4) Our results showed that the highest electron mobility was obtained for epilayer thickness around $6\sim 8 \text{ }\mu\text{m}$, and the lowest electron concentration was obtained for epitaxial thickness around $5\sim 6 \text{ }\mu\text{m}$; the results further indicated that for film thickness less than $5 \text{ }\mu\text{m}$, the electron mobility decreases drastically with decreasing epilayer thickness, implying that lattice mismatching and interfacial layer effects between GaAs substrate and the InAsP epilayer become eminent in controlling the electron mobility as well as carrier density. (5) Negative magnetoresistance was observed for this set of epitaxial samples at 4.2°K . It could be attributed to the impurity hopping

conduction dominant at this temperature. (6) Optical transmission and reflectance measurements on 13 $\text{InAs}_{1-x}\text{P}_x$ epitaxial samples yielded the absorption coefficient as a function of wavelength near the fundamental absorption edge (λ from 1 μm to 4 μm); the energy band gap as a function of alloy composition was determined for these epitaxial samples.

TABLE OF CONTENTS

CHAPTER	PAGE
I. Introduction and Summary	1
II. Electron Microprobe Studies	9
2.1 Introduction	9
2.2 Sample preparation	9
2.3 Sample embedding and polishing	10
2.4 Results of Electron Microprobe Analysis for 13 InAsP epitaxial samples	12
III. Experimental Studies of Transport Properties in InAsP Epitaxial Samples	23
3.1 Resistivity and the Hall coefficient data .	23
3.2 Dependence of electron mobility on temperature and the epi-layer thickness	24
3.3 Dependence of electron concentration on temperature and the epi-layer thickness	25
3.4 Results of magnetoresistance measurements at 300°K, 77°K, and 4.2°K	26
IV. Experimental Results of the Transmission and the Reflectance Measurements in InAs _{1-x} P _x Epitaxial Samples	39
4.1 Introduction	39
4.2 Optical Transmission Measurements	40
4.3 Reflectance Measurements	42
4.4 Optical Absorption Coefficients versus Wavelength for InAs _{1-x} P _x Epitaxial Samples	43
V. Future Plans	52
VI. References	53

LIST OF FIGURES

Figure No.	Pages
1.1 Hydrogen carrier gas flow rate versus epitaxial layer thickness for seven $\text{InAs}_{0.65}\text{P}_{0.35}$ epitaxial samples .	6
1.2 An enlarged photograph (128 X) shows the surface of an InAsP epitaxial sample.	7
1.3 An enlarge photograph (640 X) shows the surface of an InAsP epitaxial sample.	8
2.1 Coating of InAsP epitaxial samples.	15
2.2 Nickel plated InAsP samples embedded in the copper filled DIALLYL PHTHALATE.	16
2.3 Photograph of enlarged cross sectional view for samples 151 and 156	17
2.4 Relative intensity of indium, arsenic and phosphorus scanned by Electron Microprobe across the substrate, epi-layer and the nickel coating layer for samples 148, 149, 150, 151, 152, 155, 156, 157, 158 and 159.	18-22
3.1 Resistivity versus inverse temperature for six $\text{InAs}_{0.65}\text{P}_{0.35}$ epitaxial samples	29
3.2 Hall coefficient versus inverse temperature for six $\text{InAs}_{0.65}\text{P}_{0.35}$ epitaxial samples	30
3.3 Electron mobility versus inverse temperature for $\text{InAs}_{0.65}\text{P}_{0.35}$ epitaxial samples	31
3.4 Electron mobility versus epitaxial layer thickness for $\text{InAs}_{0.65}\text{P}_{0.35}$ samples	32
3.5 Electron concentration versus inverse temperature for $\text{InAs}_{0.65}\text{P}_{0.35}$ epitaxial samples	33
3.6 Electron concentration versus epitaxial layer thickness for $\text{InAs}_{0.65}\text{P}_{0.35}$ samples	34

3.7	Hall coefficient versus magnetic flux density for six InAs _{0.65} P _{0.35} epitaxial samples at T=77°K	35
3.8	Magnetoresistance versus square of the magnetic field for four InAs _{0.65} P _{0.35} epitaxial samples. . . .	36
3.9	Magnetoresistance versus square of the magnetic field for five InAs _{0.65} P _{0.35} epitaxial samples. . . .	37
3.10	Magnetoresistance versus square of the magnetic field for five InAs _{0.65} P _{0.35} epitaxial samples. . . .	38
4.1	Beam condensor attachment to Perkin-Elmer Model-98 for reflectance and transmission measurements	45
4.2	The reflectance versus wavelength for InAs, GaAs and InP	46
4.3	The absorption coefficient versus wavelength for six InAs _{1-x} P _x epitaxial samples of different alloy compositions	47
4.4	Absorption coefficient versus wavelength for seven InAs _{0.65} P _{0.35} epitaxial samples	48
4.5	Absorption coefficient versus wavelength for seven InAsP epitaxial samples with different H ₂ flow rates	50
4.6	Energy band gap versus alloy composition for 13 InAs _{1-x} P _x epitaxial samples	51

LIST OF TABLES

Table No.	Page
1.1 Epitaxially grown $\text{InAs}_{1-x}\text{P}_x$ samples produced by vapor-phase techniques used in the present study. . .	5
2.1 Tabulated data for $\text{InAs}_{1-x}\text{P}_x$ epitaxial samples (147 through 159) obtained from Electron Microprobe Analysis.	14

I. INTRODUCTION AND SUMMARY

This second semi-annual technical report covers the research activities from June to November 1974.

The purpose of this research project is to conduct experimental and theoretical studies of the basic electronic transport, recombination, impurity and defects, optical and structural properties in both bulk and epitaxial InAsP samples for the 1-2 μm infrared (IR) photocathode program and other IR devices and system applications.

Specific material parameters to be determined from this research program include: (1) electron mobility and concentration as a function of alloy composition and temperature; (2) electron lifetimes as a function of alloy composition and temperature; (3) absorption coefficient as a function of alloy composition, temperature and wavelength; (4) energy band gap versus alloy composition; (5) impurity and defect energy levels; (6) correlations between the aforementioned parameters and the epitaxial growth conditions; and (7) recombination and scattering mechanisms.

Experimental tools employed include: (1) Electron Microprobe Analysis; (2) resistivity and Hall effect measurements; (3) magnetoresistance measurements; (4) photoconductivity and photomagnetolectric effect measurements; (5) optical transmission and reflectance measurements.

Major achievements derived during this reporting period include:

(A) Preparation of 14 epitaxial samples:

During this research period, fourteen additional $\text{InAs}_{0.65}\text{P}_{0.35}$ epitaxial films have been prepared at AFCRL. These samples all have epilayers of InAsP deposited on the semi-insulating (10^6 - 10^8 ohm-cm) Cr-doped GaAs substrates. The AsH_3/PH_3 ratio used was identical to that used to grow InAsP samples 153-159 reported previously.⁽¹⁾ All growth parameters except the H_2 flow rate were held constant.

The samples were divided into two sets (see Table 1.1). One set contains samples 164, 168, 166, 169, 167, 170 and 171. The deposition time for these samples was 20 minutes. Because of varying H_2 flow rate, the resulting epilayer thickness in these samples was found to vary from 10 μm to 4 μm (see Fig.1.1).

The second set of samples contains InAsP 172, 173, 174, 175, 176, 177 and 178. These samples were deposited for six minutes and the epilayer thickness is estimated to be equal to or less than 2 μm .

It is worth noting that the quality of epilayers in these samples appeared to be much improved over our previous set of samples 153-159.⁽¹⁾ This was indeed verified from our transport measurements for samples 164-171. Fig. 1.2 and 1.3 show respectively a magnified photograph of the surface of the epitaxial film 169.

(B) Electron Microprobe Studies:

Electron microprobe analysis was performed for 13 InAs_{1-x}P_x epitaxial samples (147-159). The alloy compositions (i.e., the atomic percentages of indium, arsenic and phosphorus), the epitaxial layer thickness and the homogeneity of the epilayer were determined for these samples. The results of this analysis were summarized in Table 2.1.

(C) Resistivity and Hall coefficient data:

Resistivity and Hall effect measurements were made for samples 164 through 171 as a function of temperature between 4.2°K and 300°K. Electron mobility and concentration were deduced from these data versus temperature. Correlations between the electron mobility and the epilayer thickness, and between the electron concentration and the epilayer thickness of InAs_{0.65}P_{0.35} epitaxial samples were obtained from this study. It was found that maximum electron mobility and minimum electron concentration can be obtained for an epitaxial layer thickness between 5 and 6 μm. The electron mobility decreases rapidly with decreasing epilayer thickness for film thickness less than 5 μm, while the electron concentration increases with decreasing film thickness.

(D) Magnetoresistance data:

The magnetoresistance as a function of magnetic field for samples 164 through 171 was measured at T=300°K, 77°K and 4.2°K. The results show that the magnetoresistance ($\Delta\rho/\rho_0$) is directly proportional to the square of the

magnetic field (B^2) at small magnetic field for $T=300^\circ\text{K}$ and 77°K . Negative magnetoresistance was observed for $T=4.2^\circ\text{K}$. The results at 77°K and 300°K indicate that the conduction band structure is parabolic for $\text{InAs}_{1-x}\text{P}_x$ epitaxial samples. The negative magnetoresistance observed at 4.2°K could be attributed to the impurity hopping conduction taking place at this low temperature.

(E) Optical transmission and reflectance measurements:

Optical transmission and reflectance measurements have been performed for epitaxial samples 147 through 159 for the wavelength range from $0.9\ \mu\text{m}$ to $5\ \mu\text{m}$. Optical absorption coefficient as a function of wavelength was deduced for InAsP epitaxial samples with different alloy compositions near the fundamental absorption edge. An absorption coefficient exceeding $10^3\ \text{cm}^{-1}$ was obtained for all samples near $1\ \mu\text{m}$. The energy band gap as a function of alloy composition was determined for the InAsP epitaxial samples with different alloy compositions.

TABLE 1.1 Epitaxially grown $\text{InAs}_{1-x}\text{P}_x$ samples produced by vapor-phase techniques used in the present study.

4 to 10 μm sample*	2 μm sample [†]	H_2 flow rate used (cc/min)
164	172	1780
168	173	1530
166	174	1280
169	175	910
167	176	730
170	177	570
171	178	515

*Deposition time: 20 min.

[†]Deposition time: 6 min.

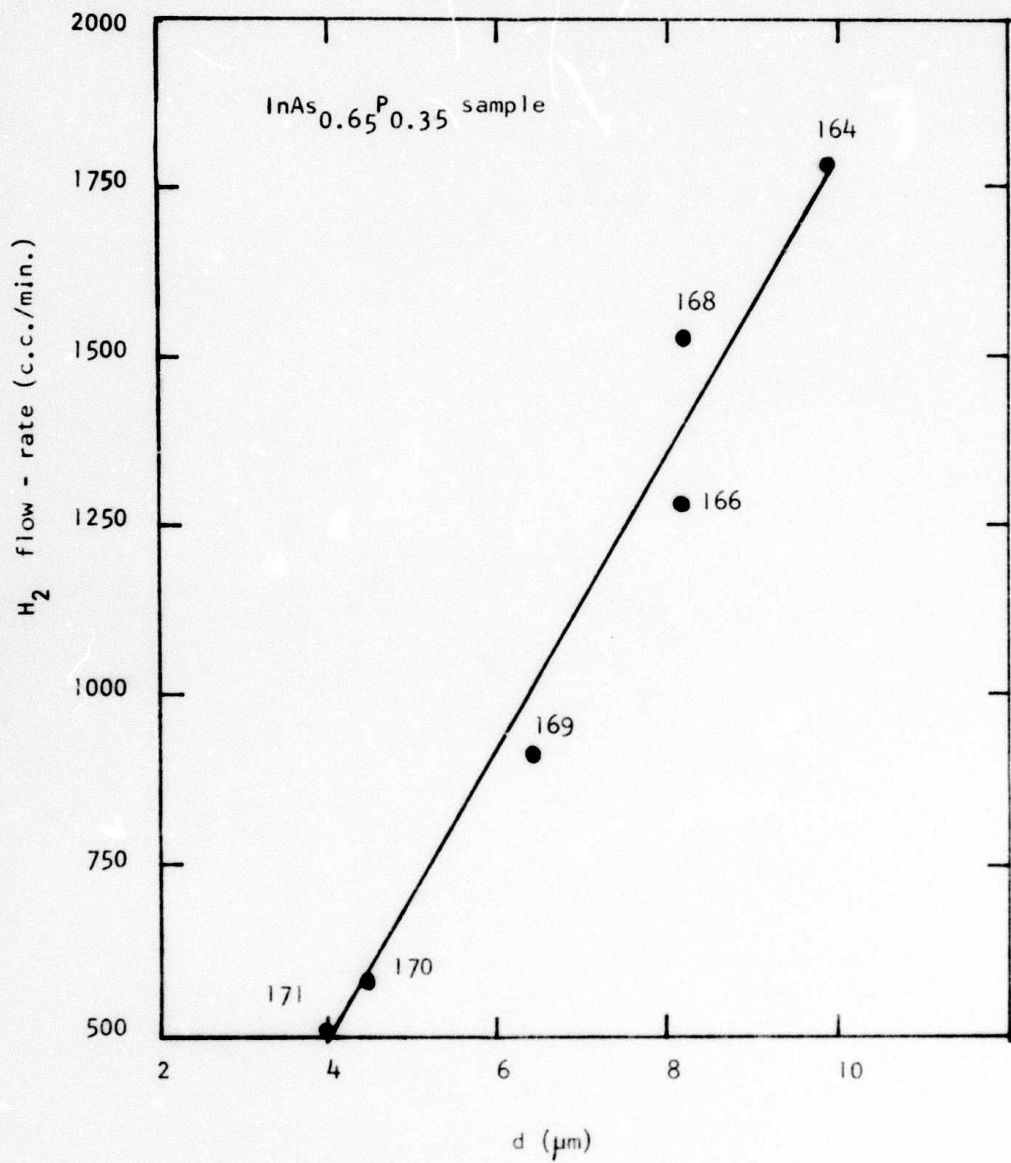


Fig. 1. | Hydrogen Flow-rate versus Epi-layer Thickness



InAsP-159

128X

Fig.1.2 An enlarged photograph for a InAsP Epitaxial sample



InAsP-169

640X

Fig. 1.3 An Enlarged Photograph (640X) shows the surface of an InAsP epitaxial sample

II. ELECTRON MICROPROBE STUDIES

2.1 Introduction

During the past six months, our ELECTRON MICROPROBE analysis has been focussed on studies of the structural properties of the epitaxially grown InAsP films deposited on the semi-insulating GaAs substrate (see Table 2.1). A technique has been developed in our Laboratory which allows a direct scanning of the cross section of the epitaxial layer by the electron microprobe. This enables us to examine the thickness, the homogeneity and the alloy composition in the epi-layer simultaneously.

The thickness of the epi-layer determined by this technique was found in good agreement with that by optical microscope method described in our previous report⁽¹⁾. Our study also showed that most of the InAsP epi-layers were uniformly grown on the GaAs substrates, and the variation in alloy composition across the epi-layer was relatively small.

2.2 Sample Preparation

In our previous work (see first semi-annual technical report, Ref. 1), only the bulk InAsP samples and the top surface of the InAsP epitaxial layers were studied by using electron microprobe technique. At that time, we

were unable to scan the cross section of the epi-layer due to the rounding of epi-layer edge during the polishing (see Fig. 2.1(a)). This rounding effect made it impossible to focus on the edge of the epi-layer, and hence reliable microprobe data was not obtainable.

This problem has been coped with by coating the epi-layer with nickel (see Fig. 2.1(b)) before the sample is embedded in the copper impregnated DIALLYL PHTHALATE (see Fig. 2.2). The nickel protective coating was applied by using an electroless nickel plating solution (AB Edgemet kit No. 20-8192 from Buehler, Ltd.).

2.3 Sample Embedding and Polishing

A slight alteration of the normal metallurgical embedding procedure is required to mount these brittle samples. Also extreme care must be taken in the embedding of these samples into the copper filled DIALLYL PHTHALATE so that they were in the upright position. An Adolph Buehler Simplimet press was used to embed these samples in the mount. This provided the conductive mounting for the electron microprobe and insured all polishing steps for each sample to be identical. Fig. 2.2 shows 13 samples that were embedded in the copper filled DIALLYL PHTHALATE.

The samples were polished by attaching the formed DIALLYL PHTHALATE slug to the precision polishing jig of the IMACO MULTIPOL PRECISION POLISHING MACHINE, described in our previous report⁽¹⁾. The polishing steps

were basically the same, except that the water used previously in the abrasive slurry was replaced by glycerine. This eliminated the abrasive surface film adhering to the surface of the specimen during polishing.

The samples were polished by successively applying different grits of silicon carbide powders, aluminum oxide and finally the glycerine damped microcloth.

It has also been found that the chemical polish sold by Materials Development Corporation called Mirrolite could produce a textureless surface on the epitaxially grown InAsP layer in the few cases tried. Further work will be attempted to determine the feasibility of using this chemical polish in place of the 0.05 μ aluminum oxide abrasive polish.

Figs. 2.3 (a) and 2.3 (b) show the enlarged photographs of samples 151 and 156, respectively, after being embedded in DIALLYL PHTHALATE and polished. In most cases, the nickel coating was of uniform thickness, however, the uniformity depends greatly on the smoothness of the epitaxial layer surface being plated. This was shown in Fig. 2.3.(b) where the rough epitaxial layer surface produced a non-uniform nickel coating. In all cases, the epitaxial layer was clearly visible and well defined. The cracking of the epitaxial film was found in some samples as a result of the intense temperature and pressure (3000 lb per square inch) during sample embedding.

2.4 Electron Microprobe Analysis

The polished InAsP epitaxial samples, shown in Fig. 2.2, were analyzed by using a Cameca MS-64 electron microprobe described previously.⁽¹⁾

The 13 samples (147 to 159) were scanned by the 1 μ m diameter electron-beam to determine the relative X-ray intensities for the indium $L_{\alpha 1}$, arsenic $L_{\alpha 1}$ and phosphorous K_{α} characteristic radiation as a function of position along the cross section extending from the GaAs substrate to the top surface of the InAsP epitaxial layer. The data obtained from InAsP samples were compared to the standards of InAs, InP, In and As. This information was then entered into a computer program, MAGIC IV for quantitative microprobe analysis, which performed all the necessary corrections to give the mean chemical composition in atomic percentage for $\text{InAs}_{1-x}\text{P}_x$ samples. The result of this analysis is summarized in Table 2.1.

To examine the epitaxial layer thickness and homogeneity, a strip recorder was connected to the output of the electron microprobe machine, and the relative X-ray intensities for each constituent atom in the InAsP epi-layer were recorded as the electron beam was scanned across each sample. Fig.2.4(a) to (e) show the relative magnitudes of the constituent atoms, namely, the arsenic, phosphorus and indium across the epi-layer. Note that the nickel coating layer contained some phosphorus and thus showed up

in the graph. The graphs showed three distinct regions, namely, the nickel coating, the InAsP epi-layer and the GaAs substrate. The homogeneity of each of the constituent atoms in the epi-layer can also be evaluated from these graphs.

The epi-layer thickness was measured from these graphs for each sample, and the result was in good agreement with that determined from the optical microscope method (see Table 2.1) described previously.

Note that the above alloy composition data were taken at an accelerating voltage of 20 KeV, the characteristic phosphorous radiation absorbed by arsenic and indium is quite large, and the absorption correction factor will be less accurate. Further measurements will be conducted at an accelerating voltage of 10 KeV and the Indium L_{α_1} , arsenic L_{α_1} , and phosphorus K_{α} x-ray intensities will be measured. At the lower acceleration voltage the depth of penetration will be much smaller, and hence less absorption will occur, resulting in a slightly more accurate compositional analysis. It is doubtful, however, that this will cause more than a 3% change in the values already obtained for the compositional measurements.

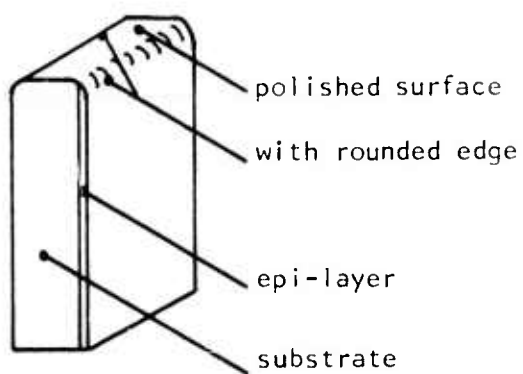
Sample	Composition in Atomic %			l-x	* x	Epitaxial Thickness by	
	In	As	P			Optical Microscope	Electron Microprobe
147	49.73	49.24	1.03	.980	.020		6.8 μm
148	51.42	44.56	4.02	.917	.083		7.9 μ
149	51.98	41.97	6.04	.874	.126		10.2 μ
150	52.24	32.92	14.84	.689	.311	† 4 - 16 μ	16.8 μ
151	53.13	22.08	24.79	.471	.529	† 7 - 25 μ	21.2 μ
152	56.92	17.25	25.83	.400	.600	21.33 μ	21.8 μ
153	50.99	31.93	17.07	.652	.348	10.40 μ	9.6 μ
154	54.67	30.88	14.45	.681	.319	10.80 μ	10.6 μ
155	49.71	33.08	17.21	.658	.342	30.73 μ	26.7 μ
156	50.31	33.60	16.09	.676	.324	22.67 μ	23.6 μ
157	51.65	32.85	15.50	.679	.321	17.33 μ	16.9 μ
158	49.53	34.70	15.77	.688	.312	14.67 μ	15.2 μ
159	47.40	35.38	17.21	.673	.327	22.13 μ	22.2 μ

† thickness of the epi-layer for these two samples was uneven.

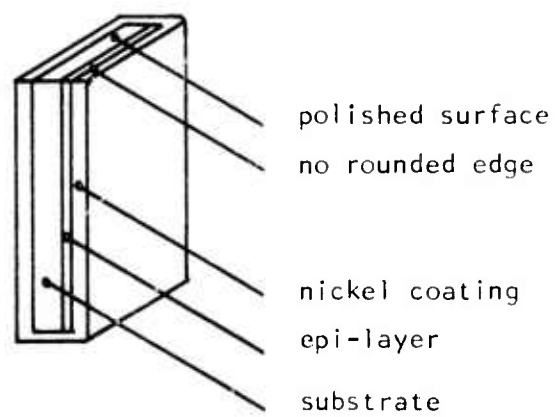
* $x = \%P / (\%As + \%P)$

‡ the average alloy composition for samples 153-159 was As=67.2% and P=32.8%

TABLE 2.1 Tabulated Data for InAs_{1-x}P_x Samples Obtained from Electron Microprobe Analysis.



(a) Without nickel coating,
shows edge rounding after
polishing



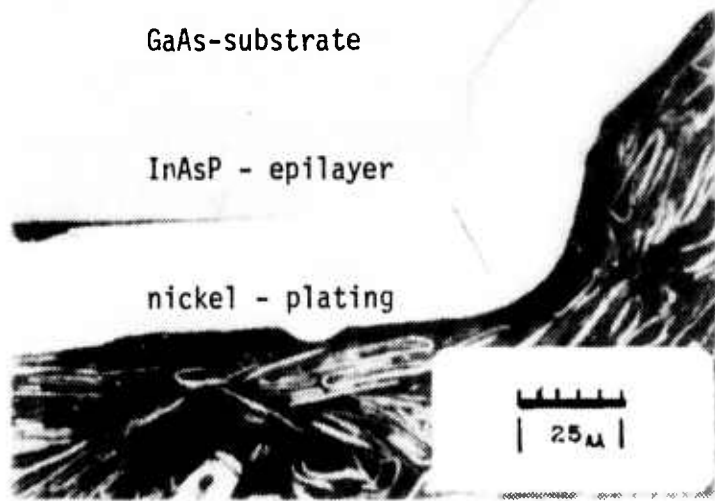
(b) Sample with nickel coating,
shows no edge rounding effect.

Fig. 2. 1 InAsP Epitaxially Grown Sample

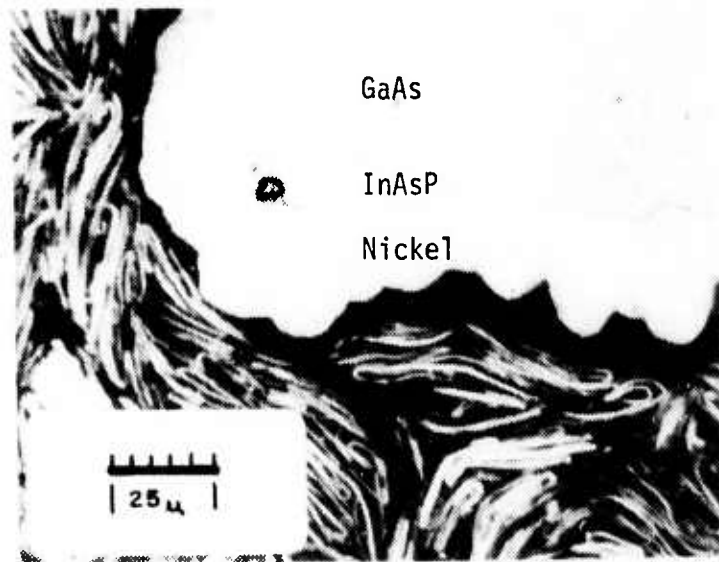


3

Fig. 2.2 Nickel Coated InAsP Samples Embedded in
Copper Filled DIALLYL PHTHALATE



(a) Sample # 151



(b) Sample # 156

Fig. 2. 3 Enlarged Cross Sectional Photograph for Samples # 151 and # 156.

Reproduced from best available copy.

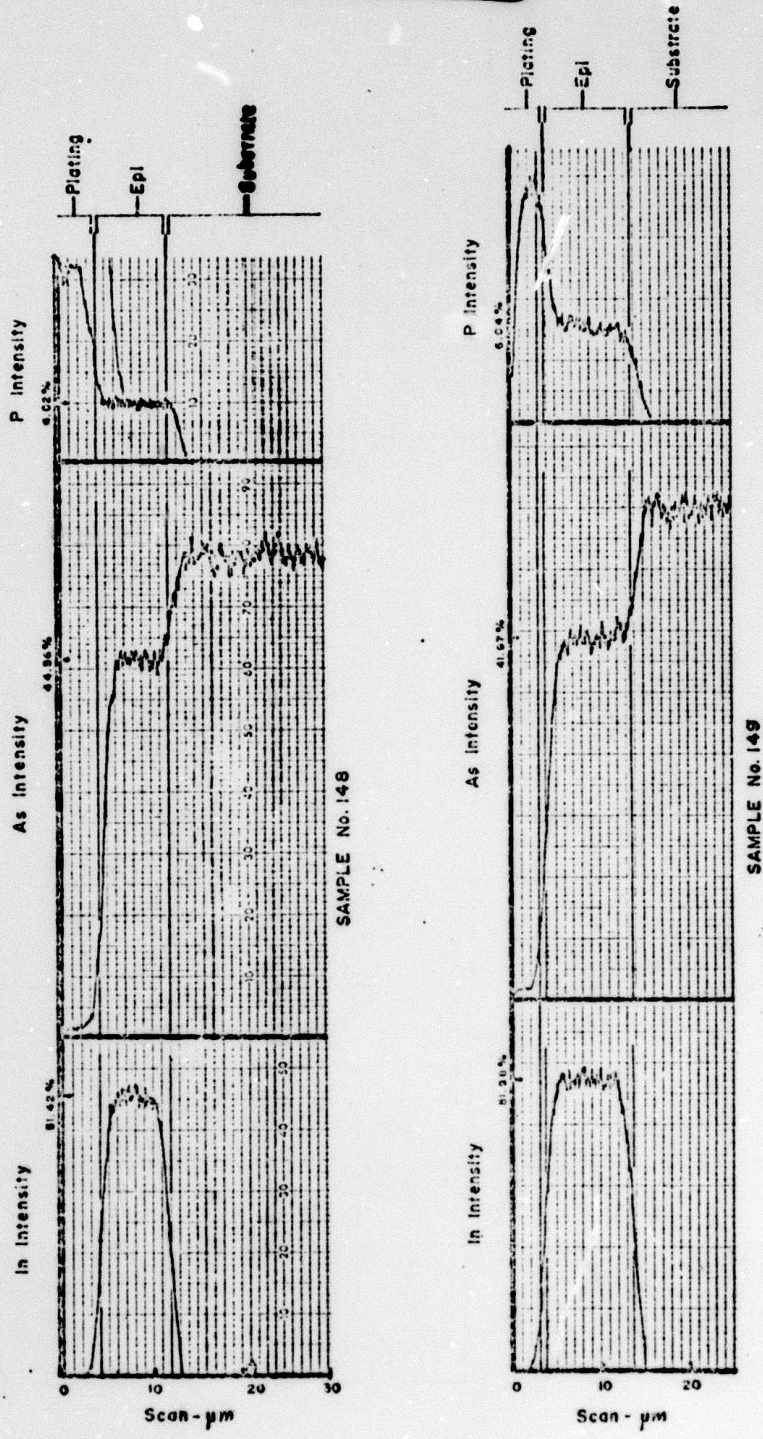


Fig. 2.4 (a) Relative Intensity of Indium, arsenic and phosphorus scanned by Electron Microprobe across the substrate, epi-layer and nickel coating for sample 148 and 149.

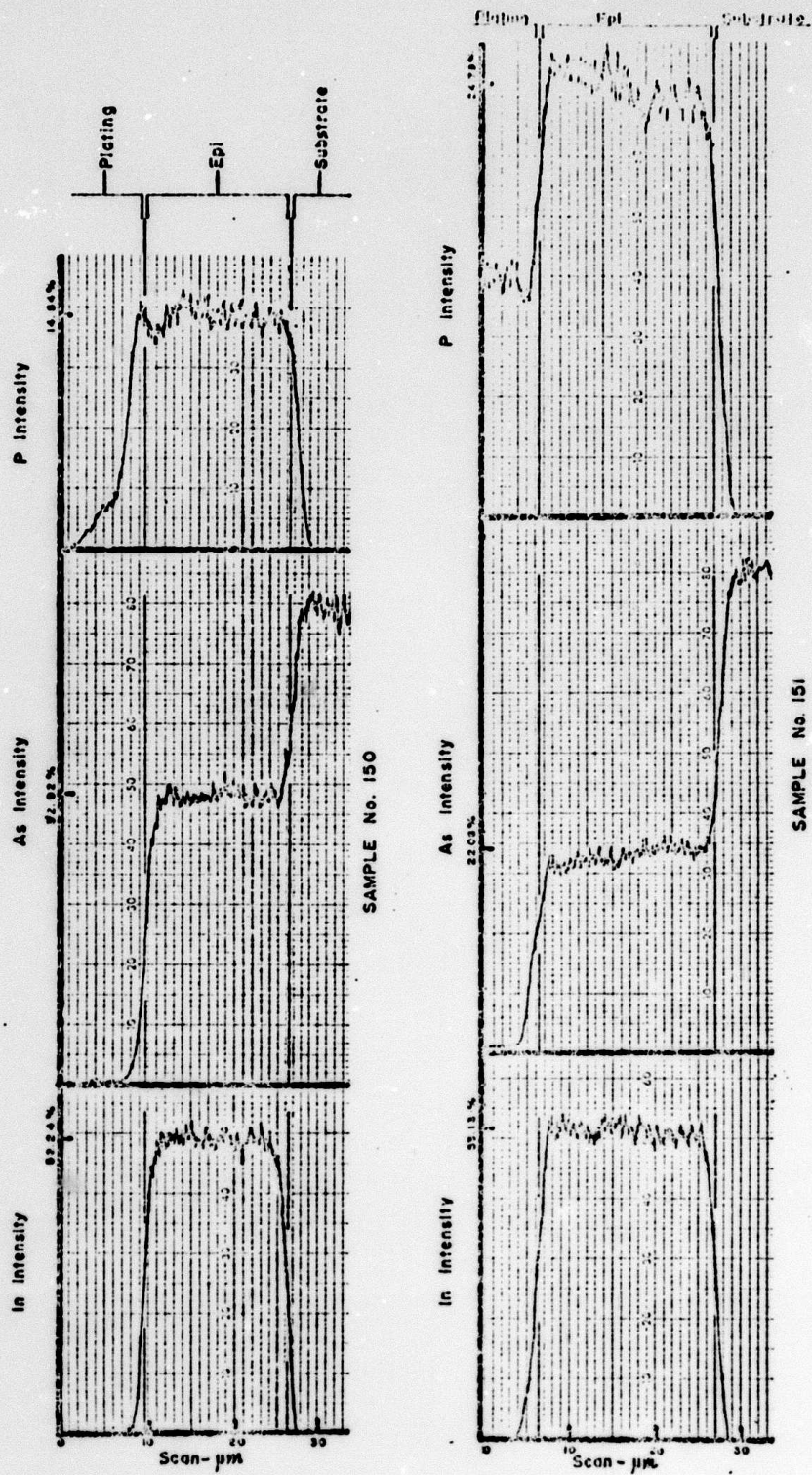


Fig. 2.4 (b)

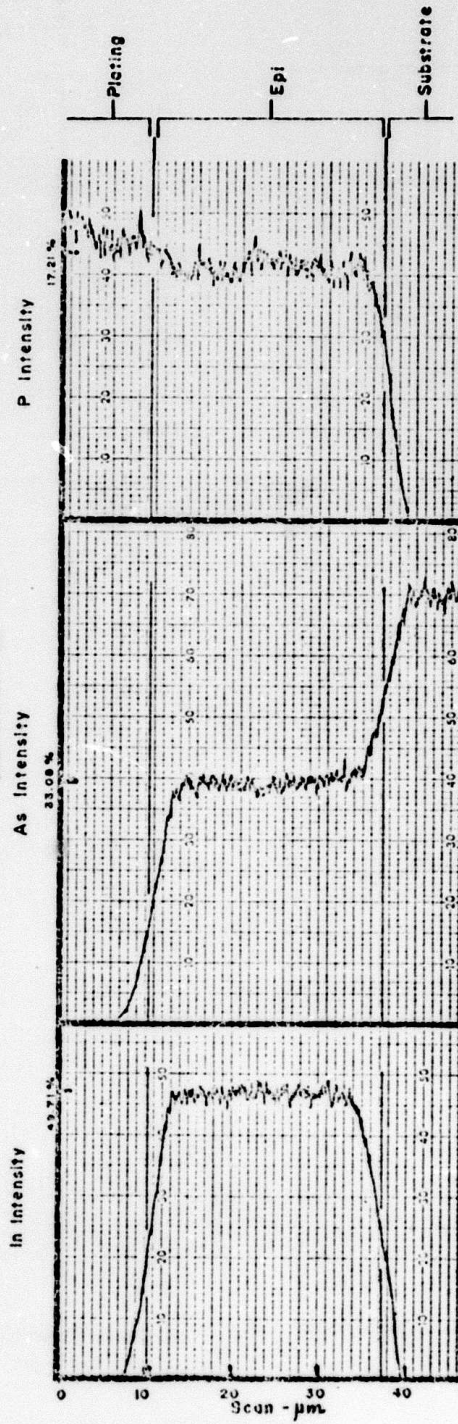
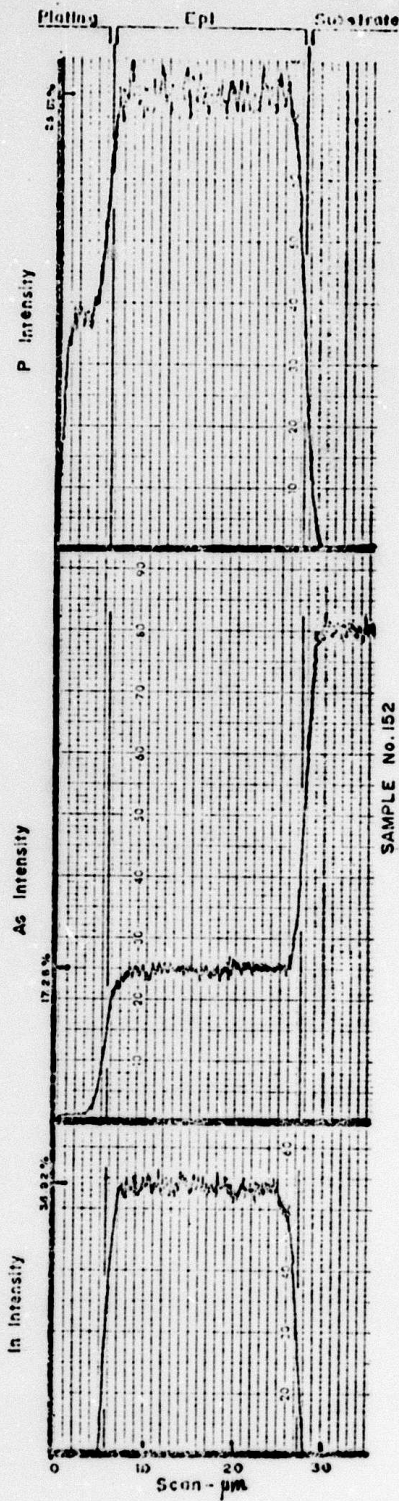


Fig. 2.4 (c)

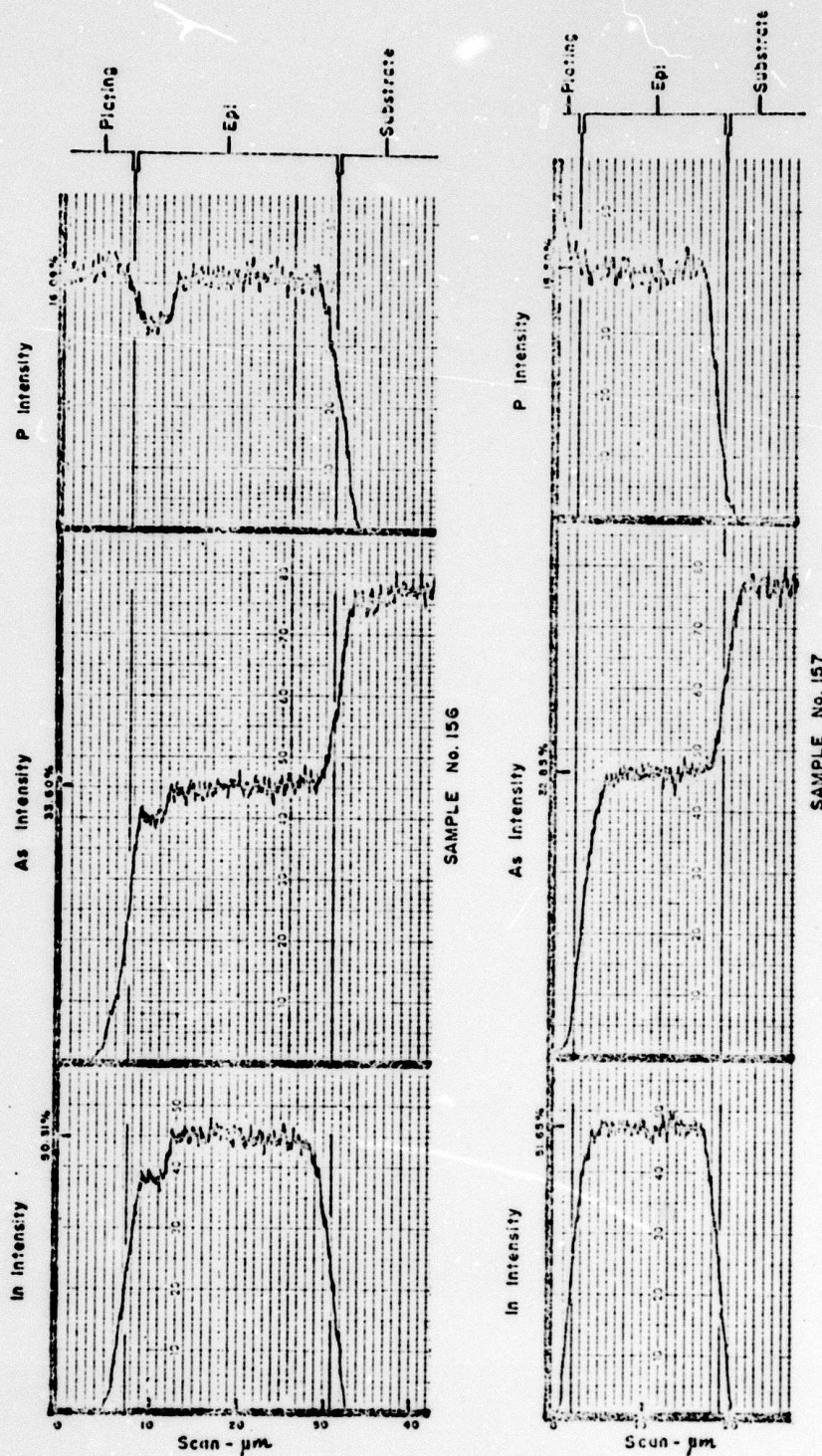
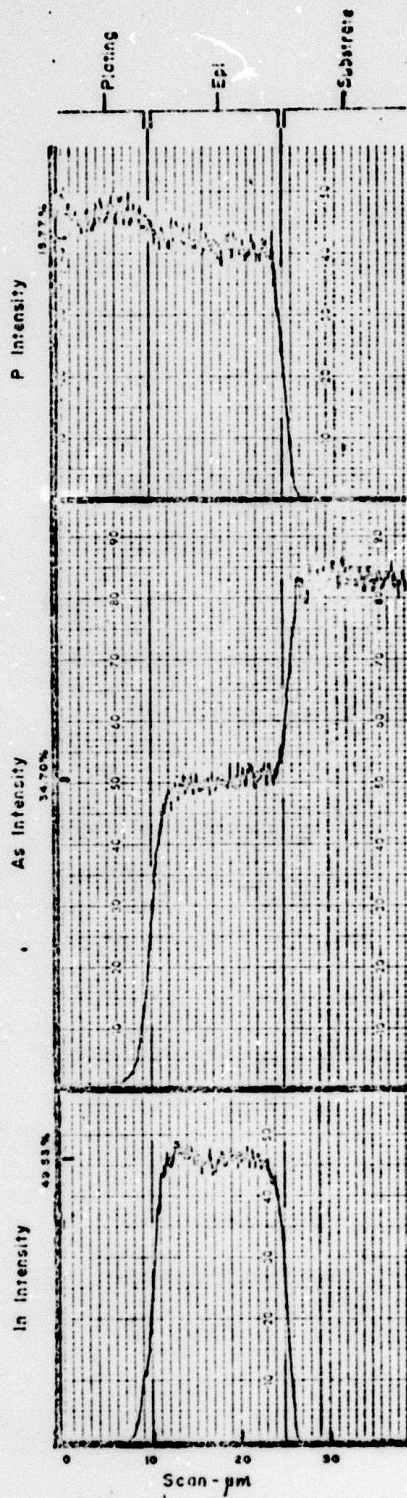
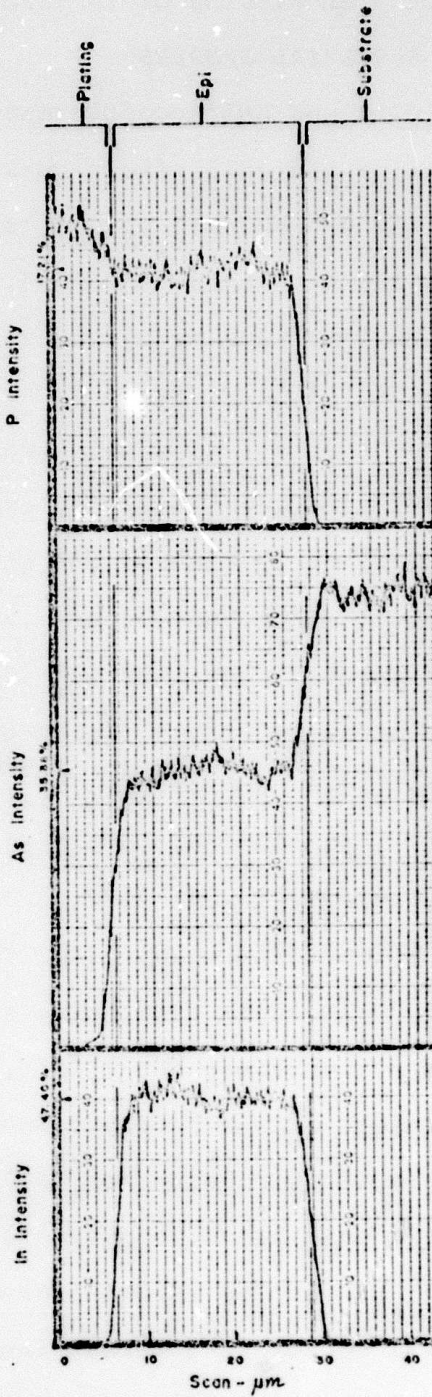


Fig. 2.4 (d)



SAMPLE No. 158



SAMPLE No. 159

Fig. 2.4 (e)

Reproduced from best available copy.

III. EXPERIMENTAL STUDIES OF TRANSPORT PROPERTIES IN

InAsP EPITAXIAL SAMPLES

3.1 Resistivity and Hall coefficient data

Resistivity and Hall effect measurements have been made for epitaxially grown $\text{InAs}_{0.65}\text{P}_{0.35}$ samples 164, 168, 166, 169, 170 and 171 between 300°K and 4.2°K. The thickness of these epitaxial films as a function of the H_2 flow rate was shown in Fig. 1.1. It is worth noting that the growth conditions for this set of samples were identical to samples 153 - 159 reported previously⁽¹⁾, except that the deposition time was reduced to 20 minutes for the present samples. As a result, the film thicknesses were varied from 10 μm to about 4 μm . However, the film quality for this set of samples was found to be considerably improved over the previous one.

Fig. 3.1 shows the resistivity versus inverse absolute temperature for samples 164 through 171. The results show that the resistivity increases with decreasing H_2 flow rate with the exception of sample 171. The resistivity increases exponentially with decreasing temperatures between 77°K and 20°K and becomes constant for $T < 20^\circ\text{K}$. The resistivity reaches a minimum around 77°K and increases exponentially with increasing temperatures for $T > 77^\circ\text{K}$. The temperature dependence for this set of samples is similar to that of the first set of samples reported previously.⁽¹⁾ Fig. 3.2 shows the Hall coefficient versus inverse absolute temperature for samples 164 through 171. The results show that the Hall

coefficient increases exponentially with decreasing temperatures for $T < 300^\circ\text{K}$, and reaches a peak around 77°K ; it then decreases exponentially for $T < 77^\circ\text{K}$ and reaches a constant value for temperatures below 20°K . This result was consistent with what we observed previously for samples 153 through 159.⁽¹⁾

The magnetic field dependence of the Hall coefficient for samples 164 through 171 is shown in Fig. 3.7 for $T=77^\circ\text{K}$. The results show that the Hall coefficient remains fairly constant over the magnetic field range from 0 to 5 kilogauss; the exception was sample 170 which shows the Hall coefficient decreasing with increasing magnetic field.

3.2 Electron Mobility

The Hall mobility was calculated from the resistivity and the Hall coefficient data shown in Fig. 3.1 and 3.2 using the relation

$$\mu_H = \sigma R_H \quad (3.1)$$

The result is illustrated in Fig. 3.3 for samples 164 through 171. It is interesting to note that the electron mobility for $T < 20^\circ\text{K}$ decreases with decreasing H_2 flow rate, indicating that the epitaxial layer thickness and the impurity compensation effect play an important role in controlling the electron mobility. To amplify this, Fig. 3.4 shows the electron mobility versus the epi-layer thickness for $T=300^\circ\text{K}$, 77°K and 4.2°K . The results indicate that the electron

mobility shows a maximum plateau for $T=300^{\circ}\text{K}$ and 77°K for film thickness around $6\sim 8\ \mu\text{m}$ and decreases drastically for film thickness less than $5\ \mu\text{m}$ and greater than $9\ \mu\text{m}$. However, for $T=4.2^{\circ}\text{K}$, the electron mobility was found to increase linearly with increasing epi-layer thickness.

The maximum electron mobility observed was $13500\ \text{cm}^2/\text{V-S}$ at 77°K , and $5300\ \text{cm}^2/\text{V-S}$ at 300°K for sample 166 (i.e., $d\approx 8\ \mu\text{m}$).

The aforementioned results lead to the conclusions that the effects of lattice mismatching and the interfacial layer between GaAs substrates and the InAsP epi-layer become important in limiting the electron mobility for film thickness less than $5\ \mu\text{m}$. For film thickness exceeding $10\ \mu\text{m}$, the electron mobility seems to be limited by the impurity scattering as reported earlier⁽¹⁾. A more thorough investigation will be conducted to study the effect of the H_2 flow rate on the electron mobility with a constant epitaxial layer thickness.

3.3 Electron Concentration

The electron concentration can be calculated from the Hall coefficient data using the relationship

$$n = \frac{\gamma}{eR_H} \quad (3.2)$$

where γ is the scattering factor varying between 1 and 2, depending upon the types of scattering processes involved.

From the results of the Hall coefficient versus magnetic field plot as shown in Fig. 3.7, we assumed that $\gamma=1$ and

calculated the electron concentration, n , from Eq. (3.2). The result is shown in Fig. 3.5. The electron concentration at 77°K was found to vary from $8.5 \times 10^{15} \text{ cm}^{-3}$ for sample 170 to $7.9 \times 10^{16} \text{ cm}^{-3}$ for sample 164, as the H_2 flow rate changes from 515 cc/min for 171 to 1780 cc/min for 164.

Fig. 3.6 shows the electron concentration versus the epi-layer thickness for samples 164 through 171 at $T=300^\circ\text{K}$ and 77°K . The results show that the lowest electron concentration obtained in this set of samples is for a sample with epi-layer thickness around $5\mu\text{m}$; the electron concentration increases with either increasing or decreasing epi-layer thickness. This could be due to both the change in the epi-layer thickness and the impurity compensation. A further study is needed to separate these two effects from each other.

3.4 Magnetoresistance Data

Transverse magnetoresistance measurements were performed for samples 164 through 171 for $T=300^\circ\text{K}$, 77°K and 4.2°K . The results are plotted in Fig. 3.8, 3.9 and 3.10. Fig. 3.8 shows $\Delta\rho/\rho_0$ versus B^2 plot for samples 169, 164, 168 and 171 at $T=300^\circ\text{K}$. A linear relationship between $\Delta\rho/\rho_0$ and B^2 was observed for four epitaxial samples for $B < 4$ kilogauss and showed saturation effects at higher magnetic field. Fig. 3.9 shows the $\Delta\rho/\rho_0$ versus B^2 at $T=77^\circ\text{K}$ for samples 166, 168, 169, 170 and 171. Again, the linear dependence of the $\Delta\rho/\rho_0$ on the square of the magnetic field (B^2) was observed for these epitaxial samples. These results led us to the con-

clusion that the conduction band structure for $\text{InAs}_{1-x}\text{P}_x$ alloys is parabolic. The magnetoresistance at low magnetic field (i.e., $\mu B \ll 1$) can be written as

$$\frac{\Delta\rho}{\rho_0} = \mu_H^2 B^2 \left[\frac{\langle \tau^3 \rangle \langle \tau \rangle}{\langle \tau^2 \rangle^2} - 1 \right] \quad (3.3)$$

We can also define the magnetoresistance coefficient, ζ , from (3.3) in the following way:

$$\zeta = \frac{\Delta\rho}{\rho_0 B^2} \cdot \frac{1}{\mu_H^2} = \frac{\langle \tau^3 \rangle \langle \tau \rangle}{\langle \tau^2 \rangle^2} - 1 \quad (3.4)$$

If we assume a nondegenerate semiconductor with an isotropic relaxation time, τ , then (3.4) reduces to

$$\zeta = \frac{\Gamma(3s + 5/2) \Gamma(s + 5/2)}{[\Gamma(2s + 5/2)]^2} - 1 \quad (3.5)$$

For acoustical phonon scattering, $s = -1/2$ and $\zeta \approx 0.275$, and for ionized impurity scattering, $s = +3/2$, and $\zeta \approx 0.57$.

The above results show that the magnetoresistance ($\Delta\rho/\rho_0$) for a nondegenerate semiconductor with spherical constant energy surface varies as B^2 at small magnetic field, and the rate of variation should be a factor of the order of unity times μ_H^2 . Both these conclusions have been observed in InAsP epitaxial samples for $T \geq 77^\circ\text{K}$ as shown in Fig. 3.8 and Fig. 3.9.

The magnetoresistance observed at 4.2°K was completely different from that of 77°K and 300°K . Fig. 3.10 shows the $\Delta\rho/\rho_0$ versus B^2 at $T = 4.2^\circ\text{K}$ for five InAsP epitaxial samples. The results show that the magnetoresistance is negative and depends strongly on the magnetic field (greater than B^2) at

low magnetic field and becomes saturated at higher magnetic field.

This negative magnetoresistance effect could be due to the impurity band conduction which was found to be the dominant mechanism at 4.2°K in these InAsP samples.⁽¹⁾ Detailed analysis of this effect will be carried out during the next reporting period.

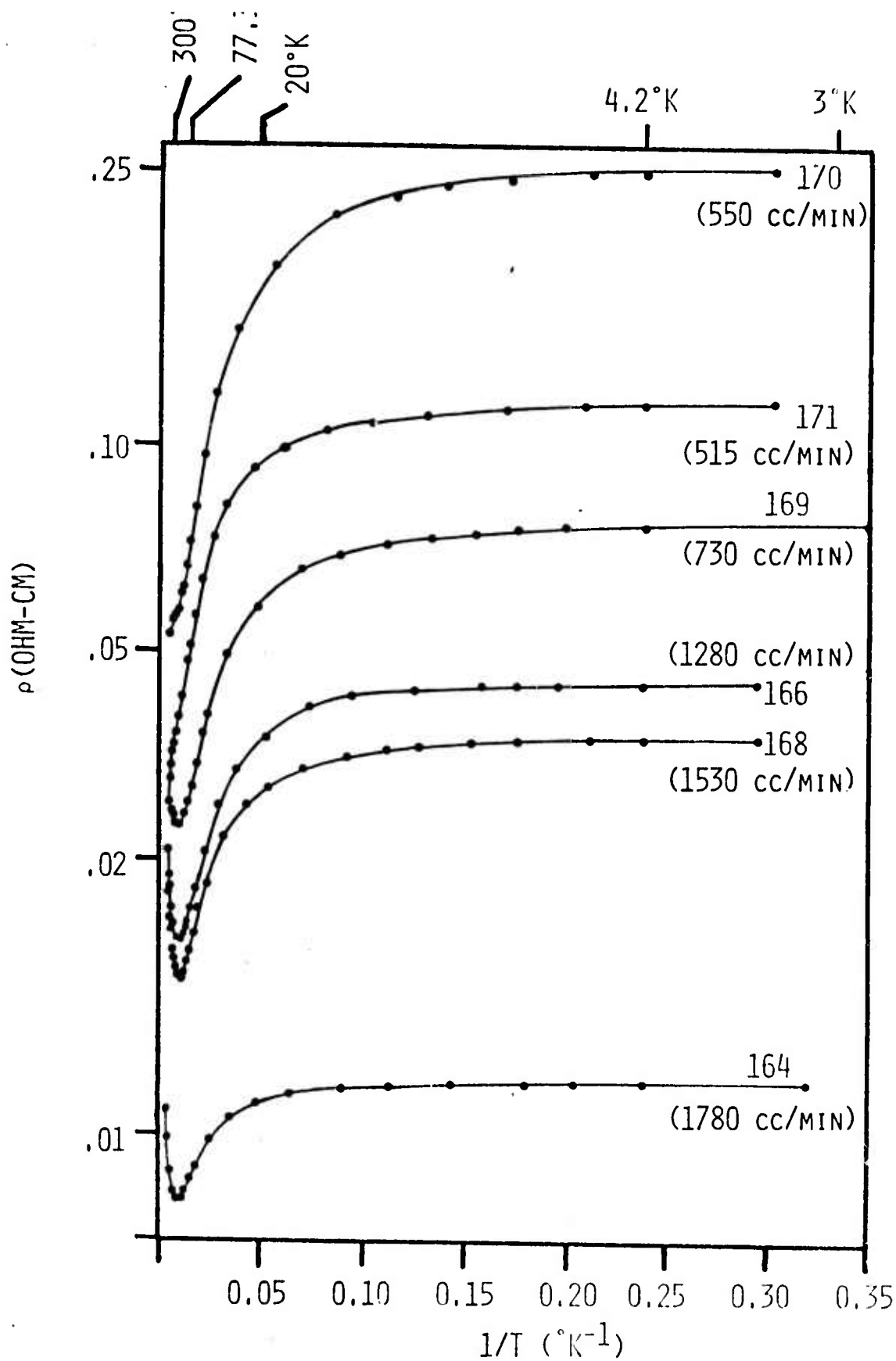


FIGURE 3.1

Resistivity versus inverse temperature for six $\text{InAs}_{0.65}\text{P}_{0.35}$ Epitaxial Samples.

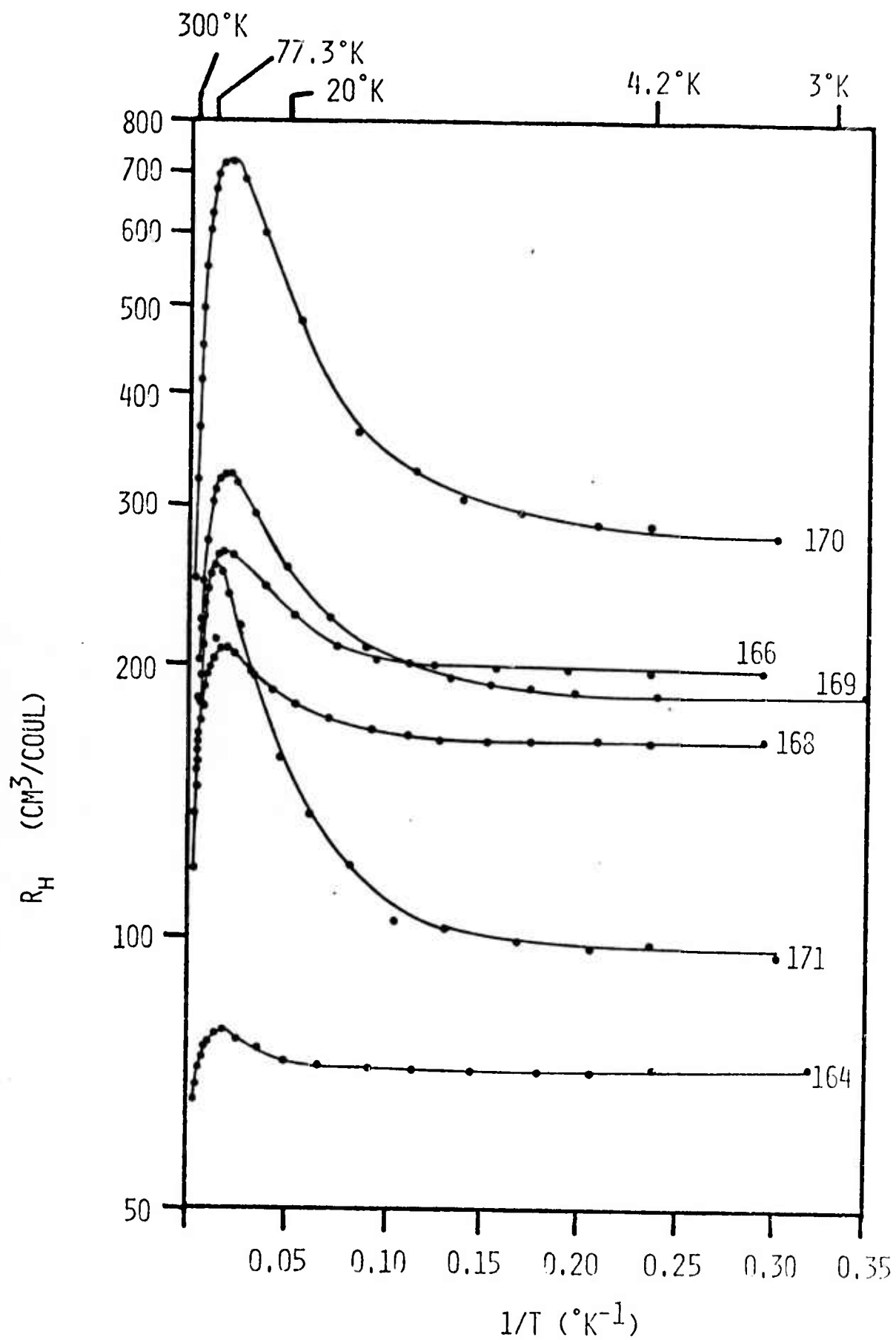
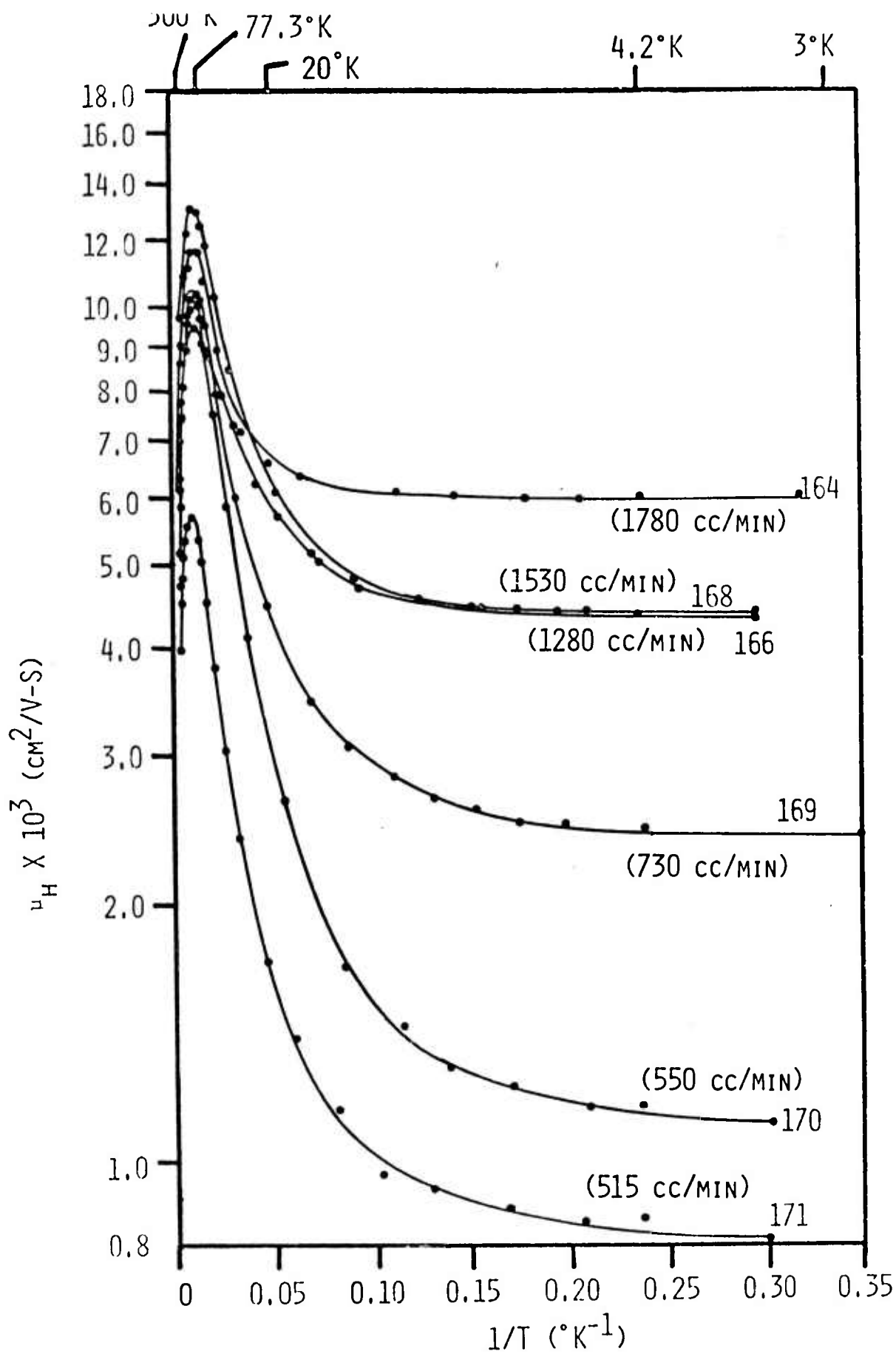


FIGURE 3.2 Hall Coefficient versus inverse temperature for $\text{InAs}_{0.65}\text{P}_{0.35}$ Epitaxial Samples.



Electron Mobility versus Inverse Temperature for InAs_{0.65}P_{0.35} Epitaxial Samples.

FIGURE 3.3.

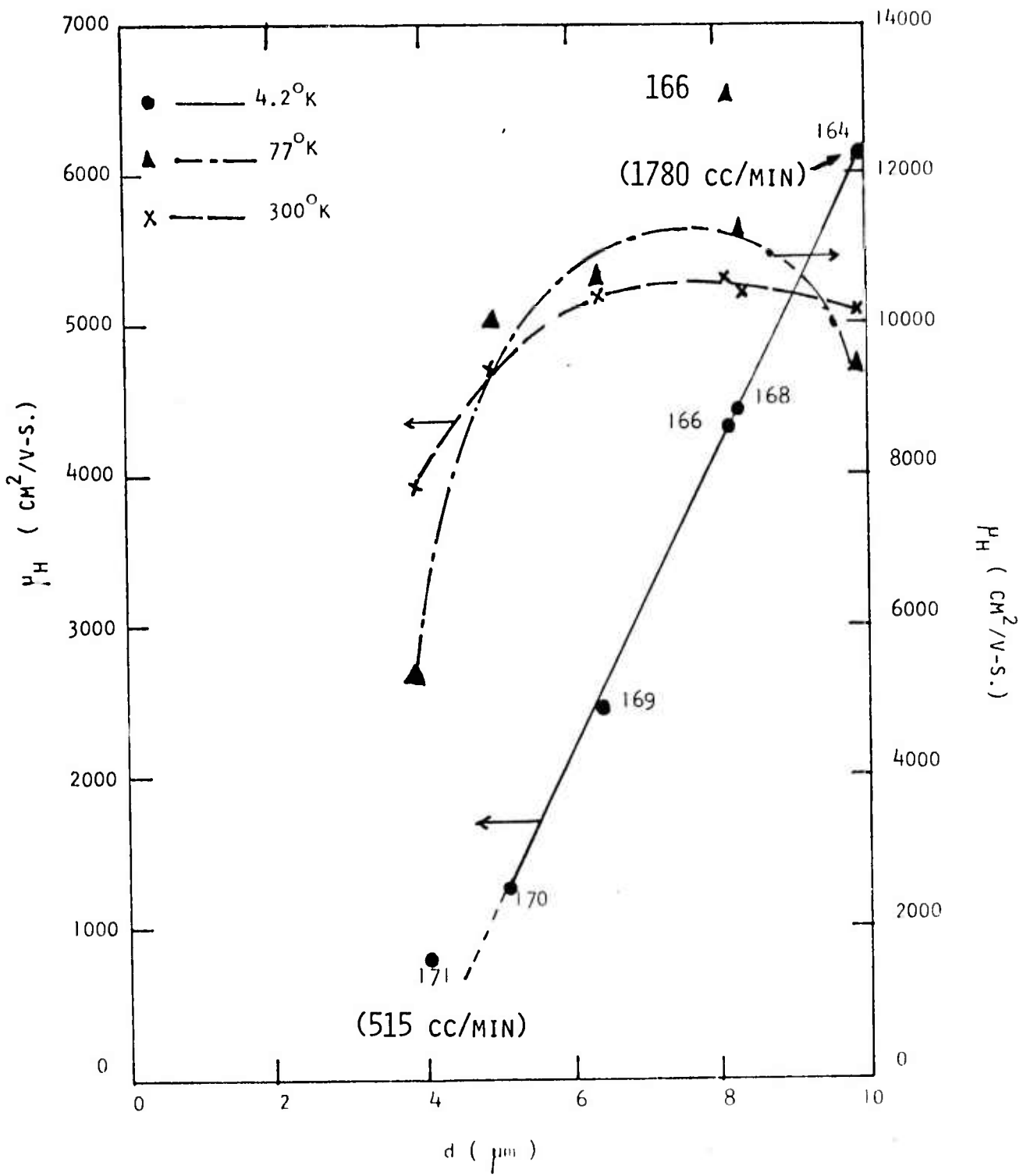


FIG. 3.4 ELECTRON MOBILITY VERSUS EPITAXIAL LAYER THICKNESS FOR $\text{InAs}_{0.65}\text{P}_{0.35}$ FILMS

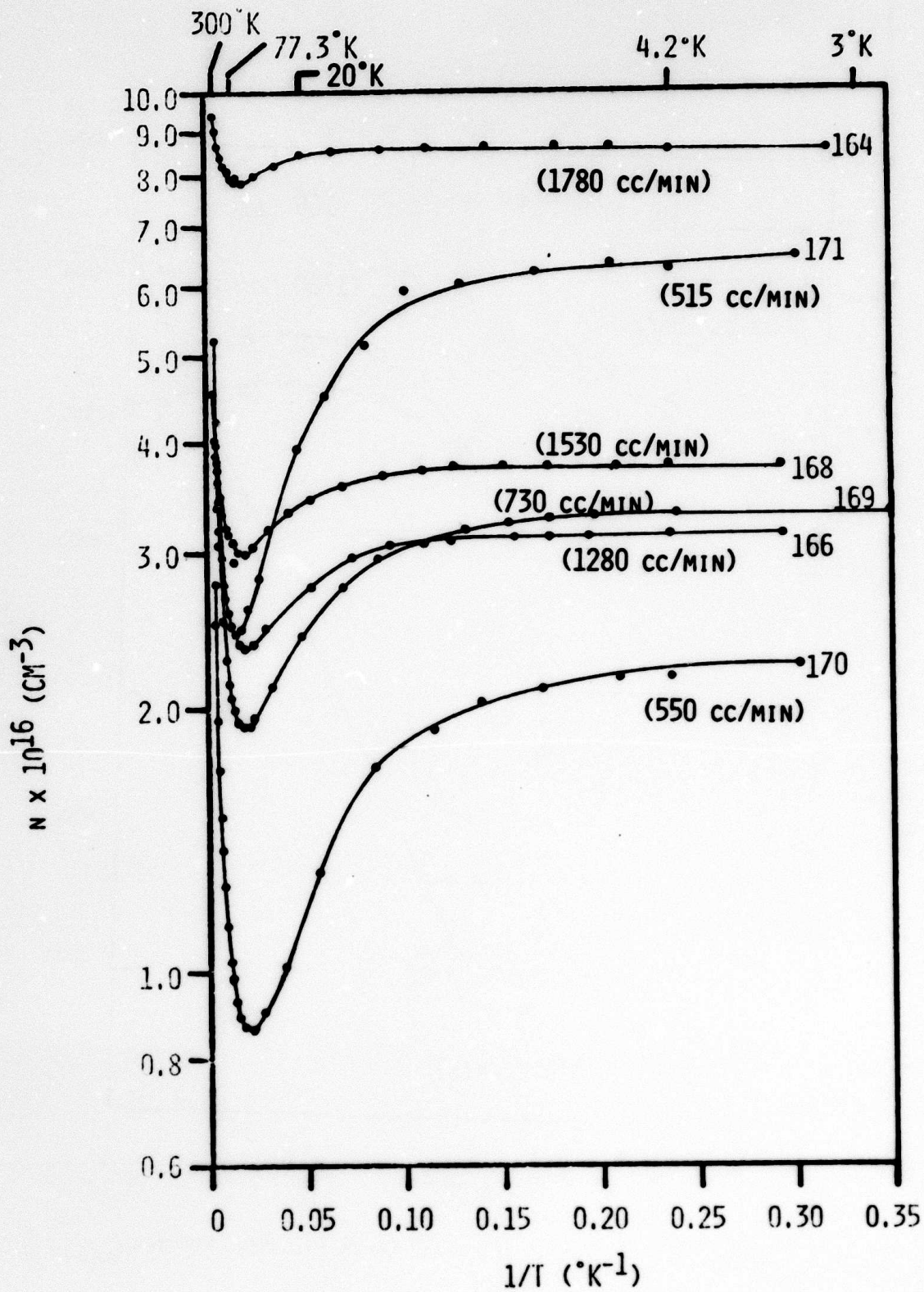


Fig. 3.5 Electron Concentration versus Inverse Temperature for Six $\text{InAs}_{0.65}\text{P}_{0.35}$ Epitaxial Samples.

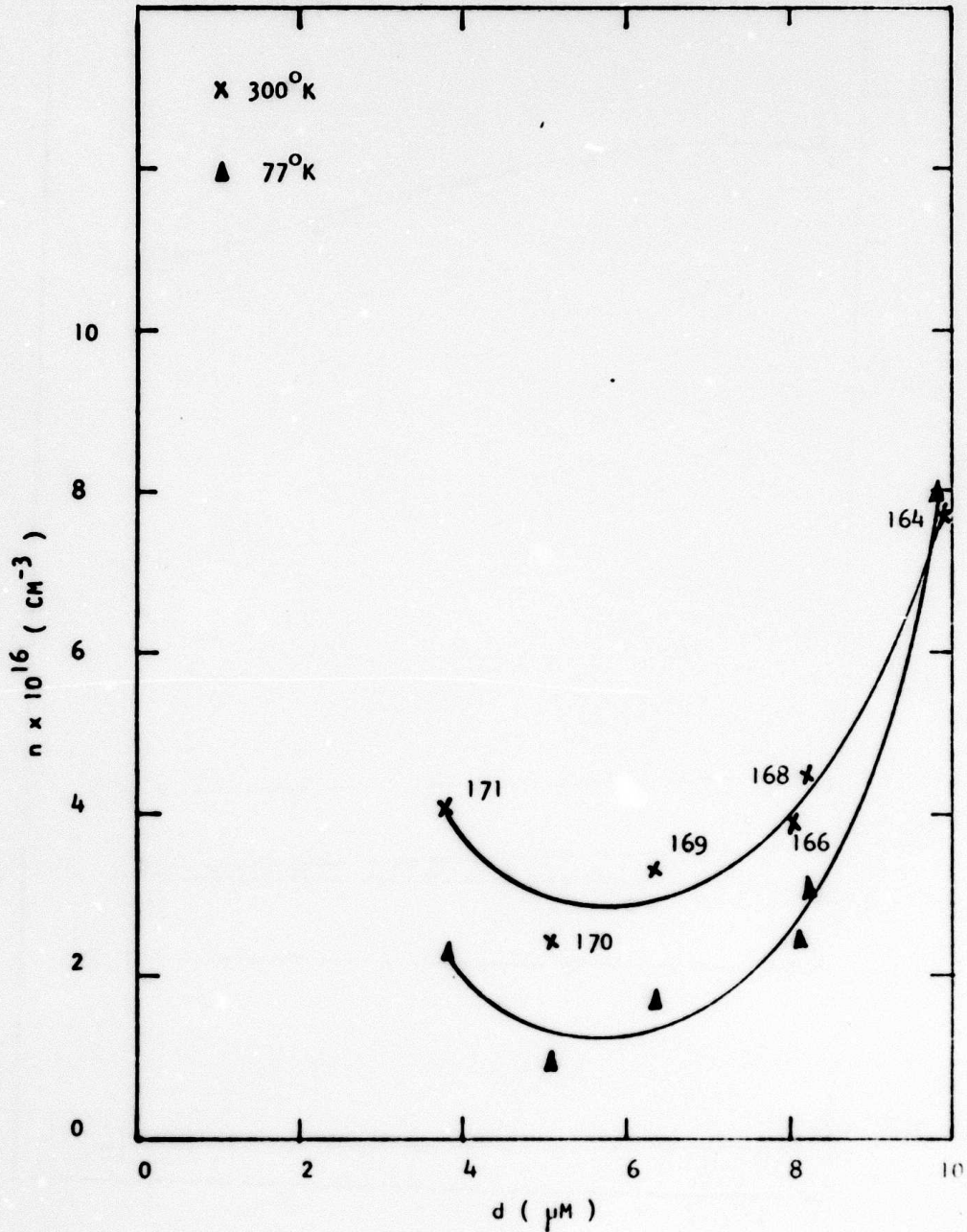


Fig.3.6 ELECTRON CONCENTRATION VERSUS EPITAXIAL LAYER THICKNESS FOR
 $\text{InAs}_{0.65}\text{P}_{0.35}$ FILMS

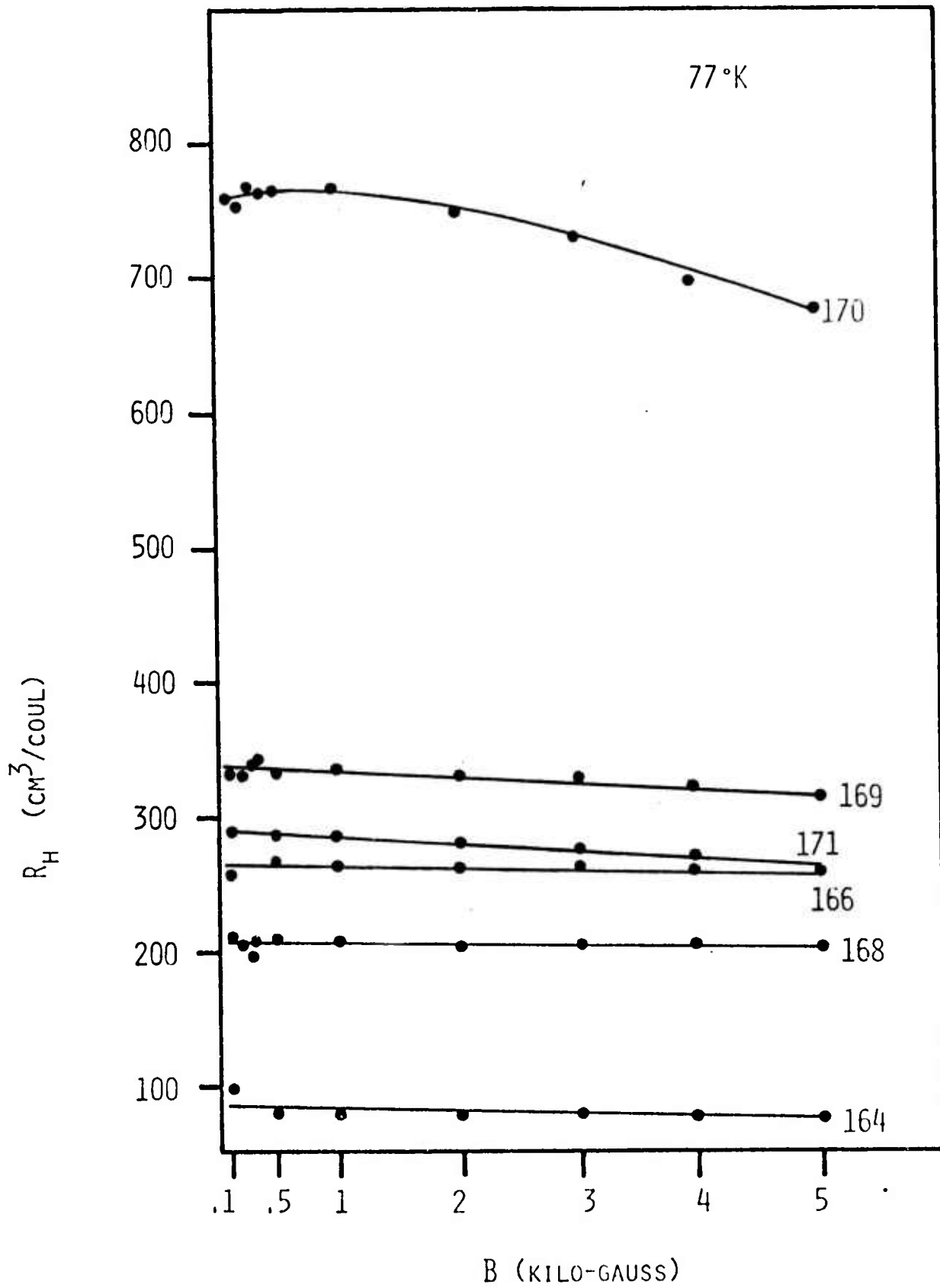


Fig. 3.7 Hall Coefficient versus Magnetic Field for $\text{InAs}_{0.65}\text{P}_{0.35}$ Epitaxial Samples.

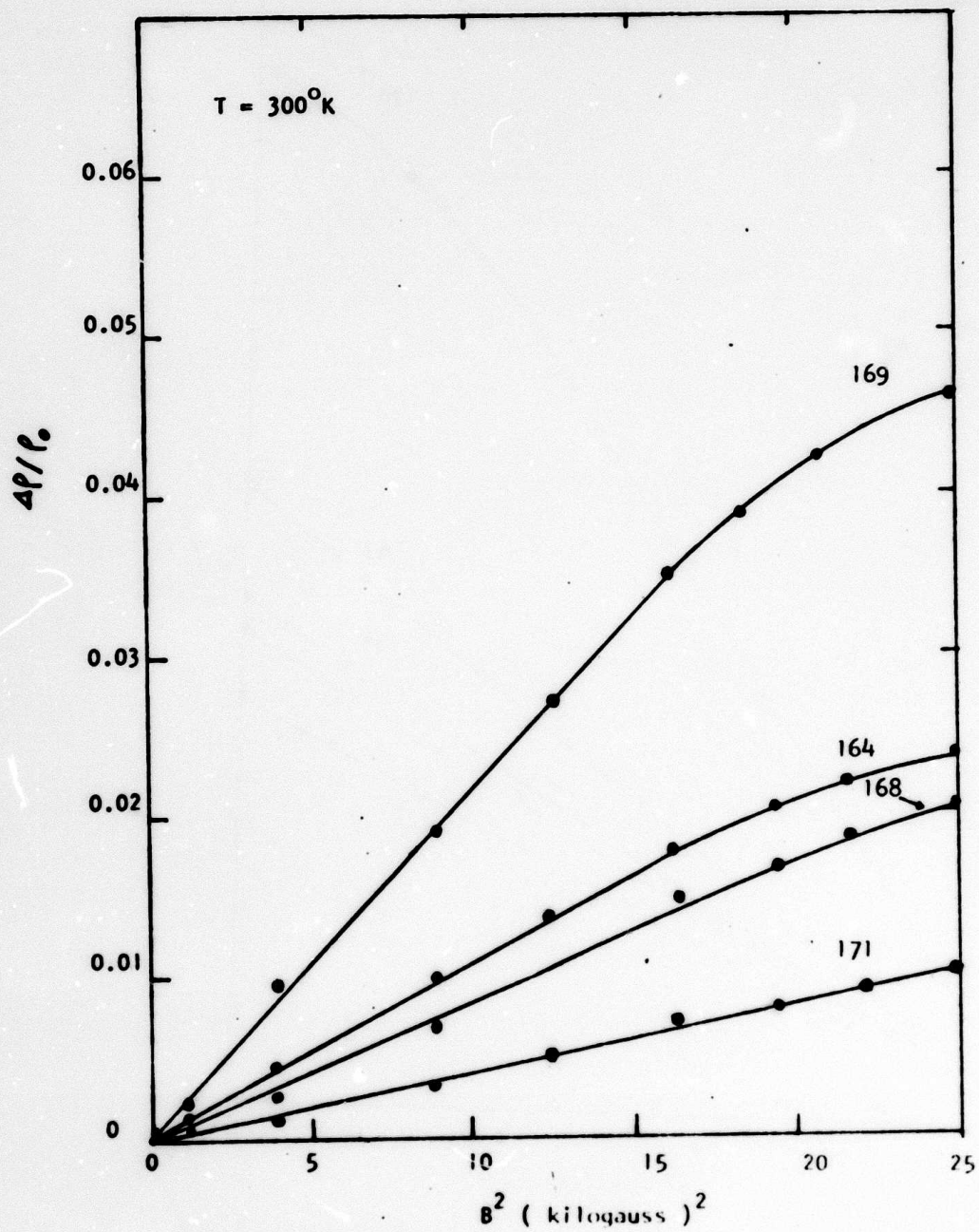


Fig.3.8 Magnetoresistance versus magnetic field square for four InAsP epitaxial samples

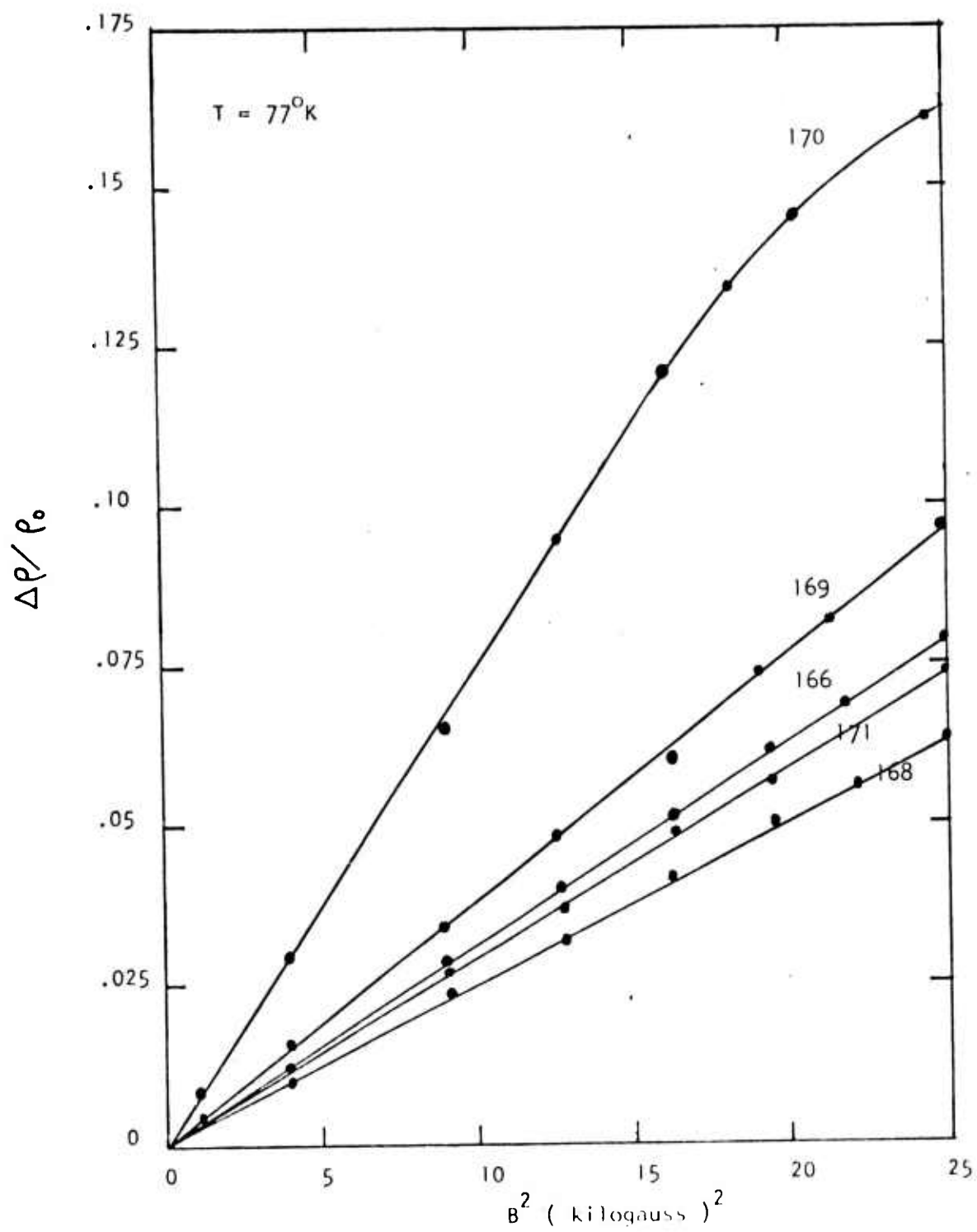


Fig. 3.9 Magnetoresistance versus square of the magnetic field for five InAsP Epitaxial samples

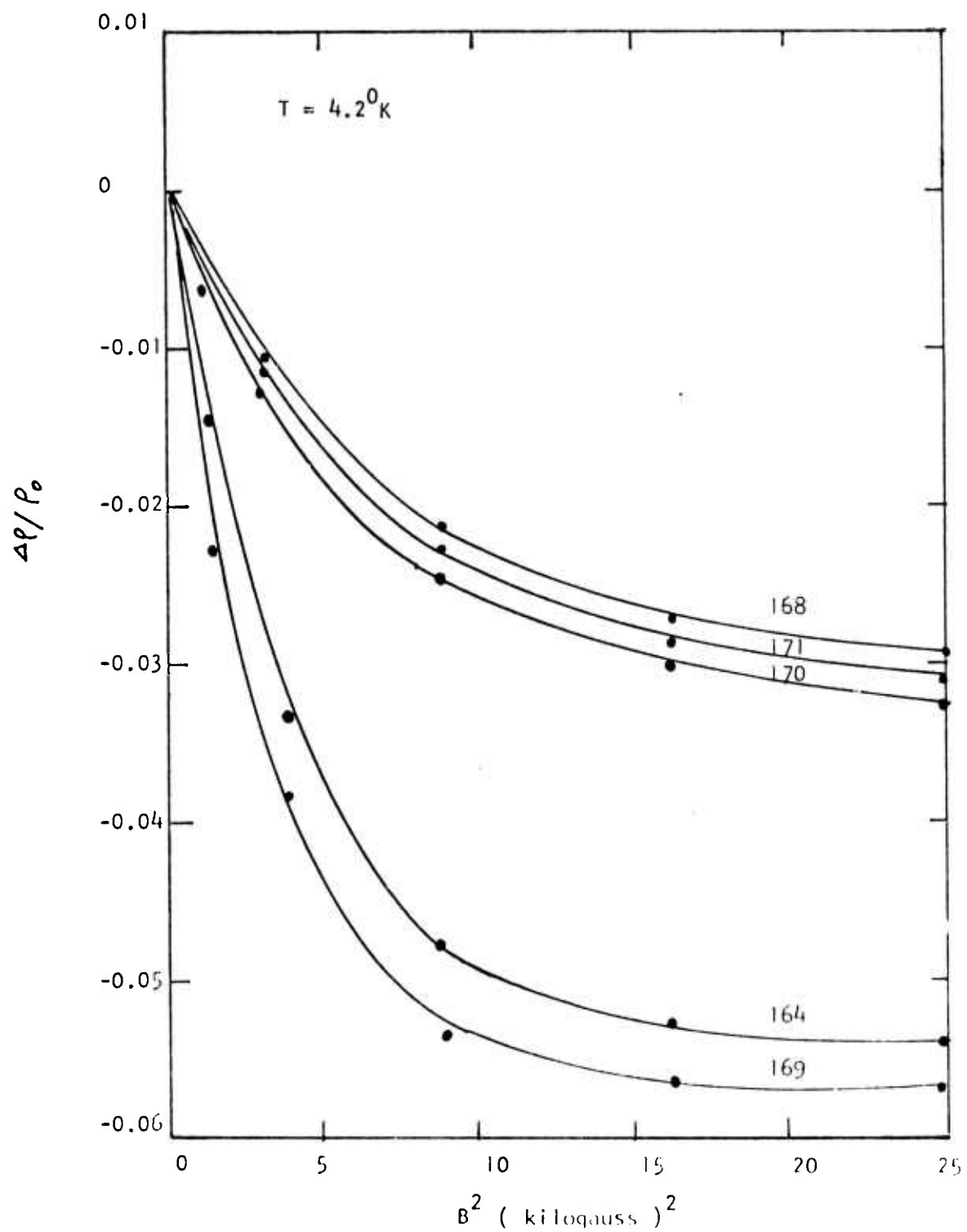


Fig.3.10 Magnetoresistance versus square of the magnetic field for six InAsP epitaxial samples.

IV. EXPERIMENTAL RESULTS OF THE TRANSMISSION AND THE REFLECTANCE MEASUREMENTS IN $\text{InAs}_{1-x}\text{P}_x$ EPITAXIAL SAMPLES

4.1 Introduction

Optical transmission measurements have been made for 13 $\text{InAs}_{1-x}\text{P}_x$ epitaxial films deposited on the semi-insulating Cr-doped GaAs substrates. The absorption coefficient as a function of the wavelength was determined for these epitaxial samples from the transmission data near the fundamental absorption edge. The energy band gap versus the alloy composition was also estimated for these epitaxial samples, and compared favorably with that obtained previously for the bulk $\text{InAs}_{1-x}\text{P}_x$ samples⁽¹⁾.

The experimental set up for the transmission and the reflectance measurements was illustrated in Fig. 4.1. A spectral reflectance unit and a 3X beam condensor attachment was incorporated into our Perkin-Elmer model-98 monochrometer (see Fig. 4.1) for the experiment. The area of the transmitted light beam was approximately 0.05 cm^2 . With this arrangement, and the fact that the epilayer thickness varies from $25 \text{ }\mu\text{m}$ to $5 \text{ }\mu\text{m}$, we were able to measure the absorption coefficient exceeding 10^3 cm^{-1} in these epitaxial samples above the fundamental absorption edge.

4.2 Optical Transmission Measurements

The study of optical absorption coefficients in $\text{InAs}_{1-x}\text{P}_x$ epitaxial samples near the fundamental absorption edge using optical transmission measurements was severely limited by the samples available and a number of unknown factors. Eliminating all of these unknown factors is highly unlikely unless destructive testing procedures are utilized. However, relative rather than absolute results still provide enough information to reach sound conclusions from these experimental measurements.

$\text{InAs}_{1-x}\text{P}_x$ epitaxial samples used for present study offered epilayer thicknesses ranging from 25 μm to about 2 μm . An absorption coefficient as high as 10^4 cm^{-1} was determined from the transmission data in these samples above the fundamental absorption edge, while bulk InAsP samples reported previously⁽¹⁾ would only allow measurement of absorption coefficients up to about 300 cm^{-1} .

The unknown factors associated with these epitaxial samples arose because the epilayers were deposited on the GaAs substrates. The thicknesses of the GaAs substrates varied from 0.020" to 0.026". It is difficult to estimate the absolute absorption coefficient in the GaAs substrate and the reflectance at the interface of InAsP epilayer and the GaAs substrate. An example to illustrate this follows:

Assuming $\lambda > 1 \mu\text{m}$, $0 < \alpha \leq 3 \text{ cm}^{-1}$, $R = 0.289$, and $d = 0.020$ ", using the expression for transmission coefficient⁽²⁾

$$t_{\text{Transmission}} = \frac{(1-R)^2 e^{-\alpha d}}{1-R^2 e^{-2\alpha d}} \quad (4.1)$$

yields $t_T=0.46252$.

This means that under the above conditions, only 46% of the light which is transmitted through the InAsP epilayer will be transmitted through the GaAs substrate. It is extremely difficult to separate the absorption in the InAsP epilayer and the GaAs substrate when the two components are comparable. Fortunately, since we are mainly concerned with locating the fundamental absorption edge, when the absorption coefficient in the $\text{InAs}_{1-x}\text{P}_x$ changes from 10^4 to 10^2cm^{-1} at the edge, this error is not great enough to obscure the experimental results.

Another limitation introduced by using the epitaxial sample is that absorption coefficients in InAsP epilayer can not be measured accurately for wavelengths shorter than $1 \mu\text{m}$ because of the GaAs substrate which has an absorption edge around $0.9 \mu\text{m}$.

It is also worth noting that the normal incidence of the light beam is more important with epitaxial samples than with the bulk samples. A light beam incident 40° from the normal to the sample plane for bulk samples appeared to be approximately equivalent to just a 5° incidence angle for the epitaxial samples. It seems that the interfacial surface between the InAsP epilayer and the GaAs substrate plays an important role in these optical measurements.

In summary, a priori results can be supported and the experimental error was estimated at about 2 ~ 3% despite these limitations.

Results of the absorption coefficients derived from the transmission data for the InAsP epitaxial samples will be discussed in Section 4.4.

4.3 Reflectance Measurements

The reflectance measurement was performed for GaAs, InAs, InP and some InAsP epitaxial samples using the experimental setup shown in Fig. 4.1. The results for GaAs, InAs and InP samples are found in good agreement with the published data⁽²⁾, as is shown in Fig. 4.2.

Although results for some InAsP samples were obtained, some discrepancy for reflectance data was found as the fundamental band edge is approached from the visible spectrum. Thus, further experimental work is planned in this area during the fifth and sixth contract period for both bulk and epitaxial InAsP samples.

In order to correct some of the problems encountered in our present reflectance measurements, we plan to add a standard reflector of known reflectance in the 0.5 eV to 10 eV region and a high power UV light source. In addition, sample surface quality must be improved by developing new polishing techniques.

A Caro acid etching solution has been used in the past for polishing InAsP samples; however, it was found that the sample surface was selectively etched. Reflectance measure-

ments have shown that in the long wavelength region the surface condition is of little importance and will change the experimental results by only a few percent.

4.4 Optical Absorption Coefficients versus Wavelength for InAs_{1-x}P_x Epitaxial Samples

In our first technical report⁽¹⁾, we have shown that a non-linear relationship between the alloy composition and the energy band gap exists in bulk InAs_{1-x}P_x samples. This relationship was again observed in our present study of epitaxial InAsP samples.

The optical absorption coefficient versus wavelength was deduced from the transmission data (discussed in Section 4.2) for 13 epitaxial InAs_{1-x}P_x samples. Fig. 4.3 shows the absorption coefficient versus wavelength for six InAs_{1-x}P_x epitaxial samples of different alloy compositions. Absorption coefficients of the order of 10^3 cm^{-1} were obtained for these samples above the fundamental absorption edge. However, it was found that the absorption coefficient appeared to decrease with increasing phosphorus atomic percentage above the fundamental absorption edge. This result could be due to the fact that as phosphorus concentration increases, the band gap of InAs_{1-x}P_x increases, shifting towards the band edge of GaAs substrate; as a result, the effect of optical absorption within GaAs substrate becomes important in controlling the overall absorption coefficient in the InAsP epitaxial samples. As such, the measured absorption co-

efficient could be well below the actual values in these epitaxial samples. However, for $\text{InAs}_{1-x}\text{P}_x$ samples with smaller phosphorus percentage, this effect should be minimum and negligible as the GaAs substrate becomes transparent. This is indeed the case for sample 147 (which has only 3% of phosphorus). It is also worth noting that the slope near the fundamental absorption edge appears to become steeper as the phosphorus atomic percentage is increased in these $\text{InAs}_{1-x}\text{P}_x$ epitaxial samples.

Fig. 4.4 shows the absorption coefficient versus wavelength for epitaxial samples 153 through 159, deduced from transmission data near the fundamental absorption edge. Presumably, this set of epitaxial samples should contain the same alloy composition (since only the H_2 flow rates were varied during the epitaxial-layer growth); it was, however, found that a variation in atomic percentage of Arsenic and phosphorus as much as 17% was observed from optical transmission data and about 5% from electron microprobe analysis. The average value of alloy compositions deduced from Fig. 4.4 is 67% As and 33% P (i.e., $\text{InAs}_{0.67}\text{P}_{0.33}$) contrasting with the original anticipated values of 61% As and 39% P. The reason is not clear at the present stage. Further study is needed.

The optical absorption coefficient versus wavelength for epitaxial samples 164 through 171 near the fundamental edge is shown in Fig. 4.5. The average alloy compositions of this set of epitaxial samples was found to be 35% of P and 65% of As. This value is about 4% lower than the anticipated values.

From the aforementioned results, the energy band gap versus the alloy composition for the 13 $\text{InAs}_{1-x}\text{P}_x$ epitaxial samples is shown in Fig. 4.5. A linear relationship between the energy band gap and the alloy composition, x , is displayed in Fig. 4.6.

Note that the optical absorption coefficient data shown in Fig. 4.4 have been corrected using the Kramers-Kronig relationship.⁽²⁾ This correction becomes important wherever $e^{-\alpha d} \geq 0.01$.

The shift in the fundamental absorption edge towards the longer wavelength region for the $\text{InAs}_{0.65}\text{P}_{0.35}$ epitaxial samples (164-171) with decreasing epilayer thickness indicates that the transition layer between GaAs substrate and InAsP epilayer is more arsenic rich than the epilayer far from this transition region. The importance of this transition layer (2 ~ 4 μm) on the transport and optical properties is clearly illustrated in Fig. 3.4, 3.5 and 4.5. Detailed study will be made in this respect during the next reporting period.

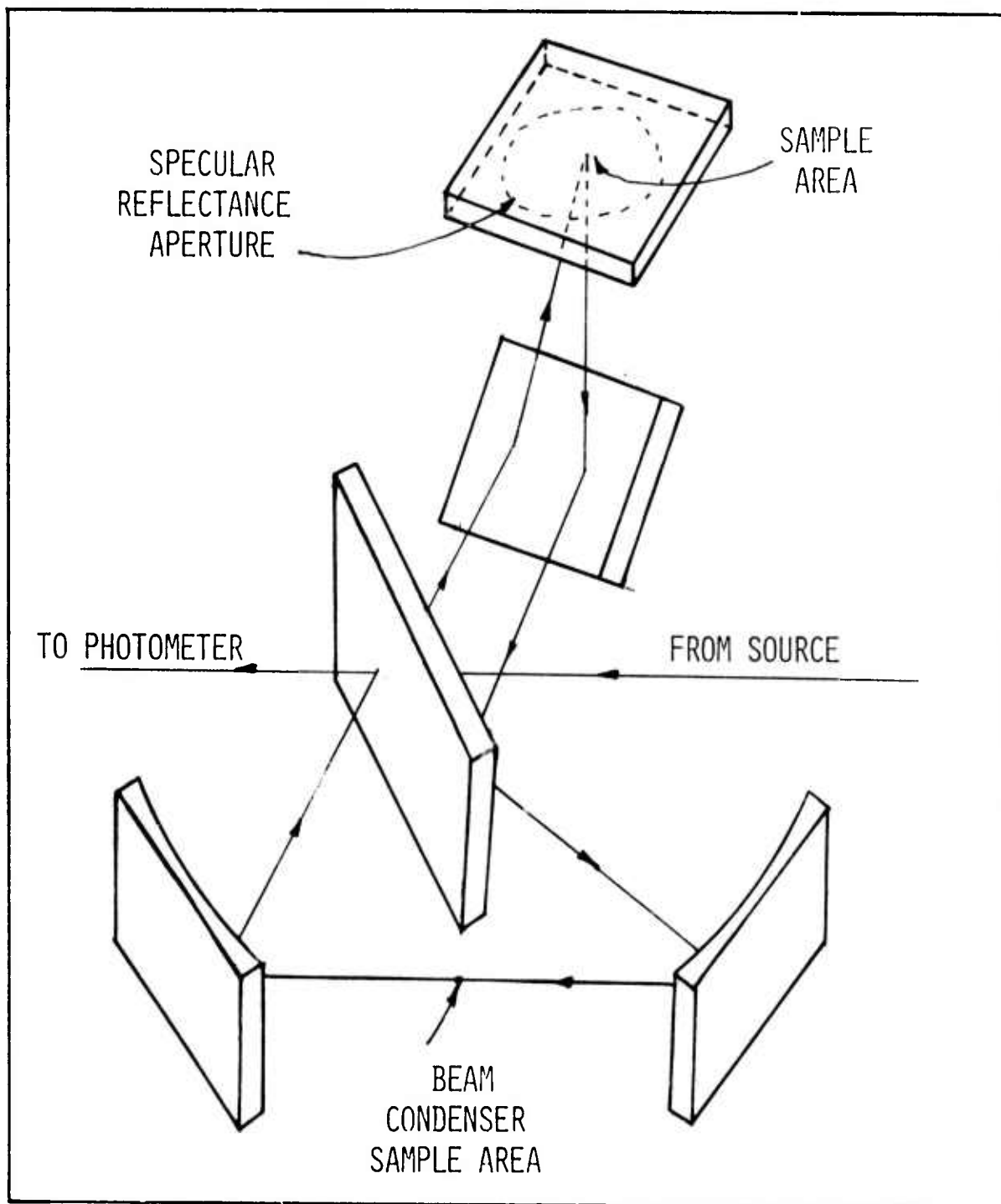


Fig. 4. 1 Beam Condenser Attachment to Perkin-Elmer Model-98 for Reflectance and Transmission Measurements

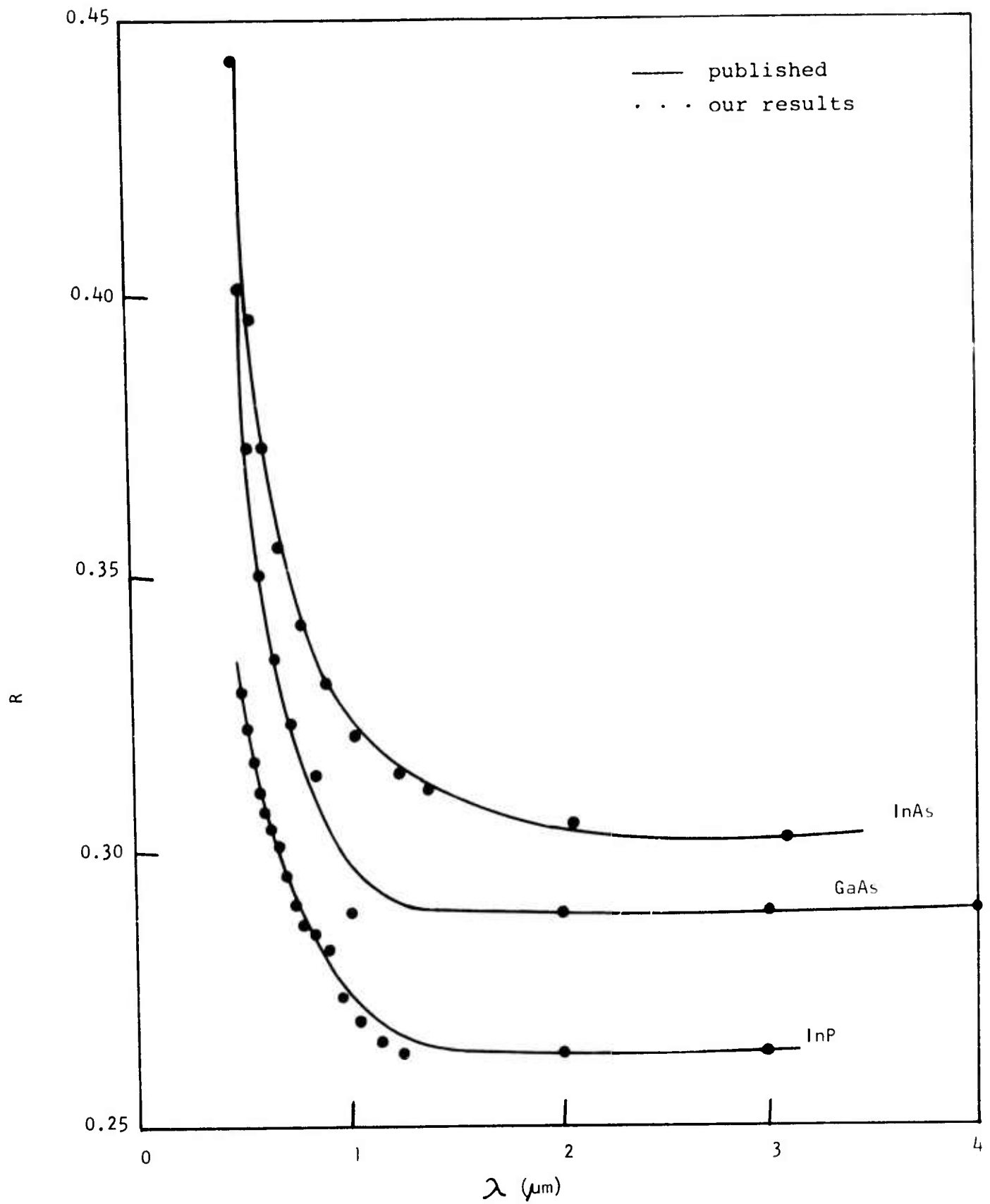


FIG. 4.2 The reflectance versus wavelength for InAs, GaAs and InP (reference 2)

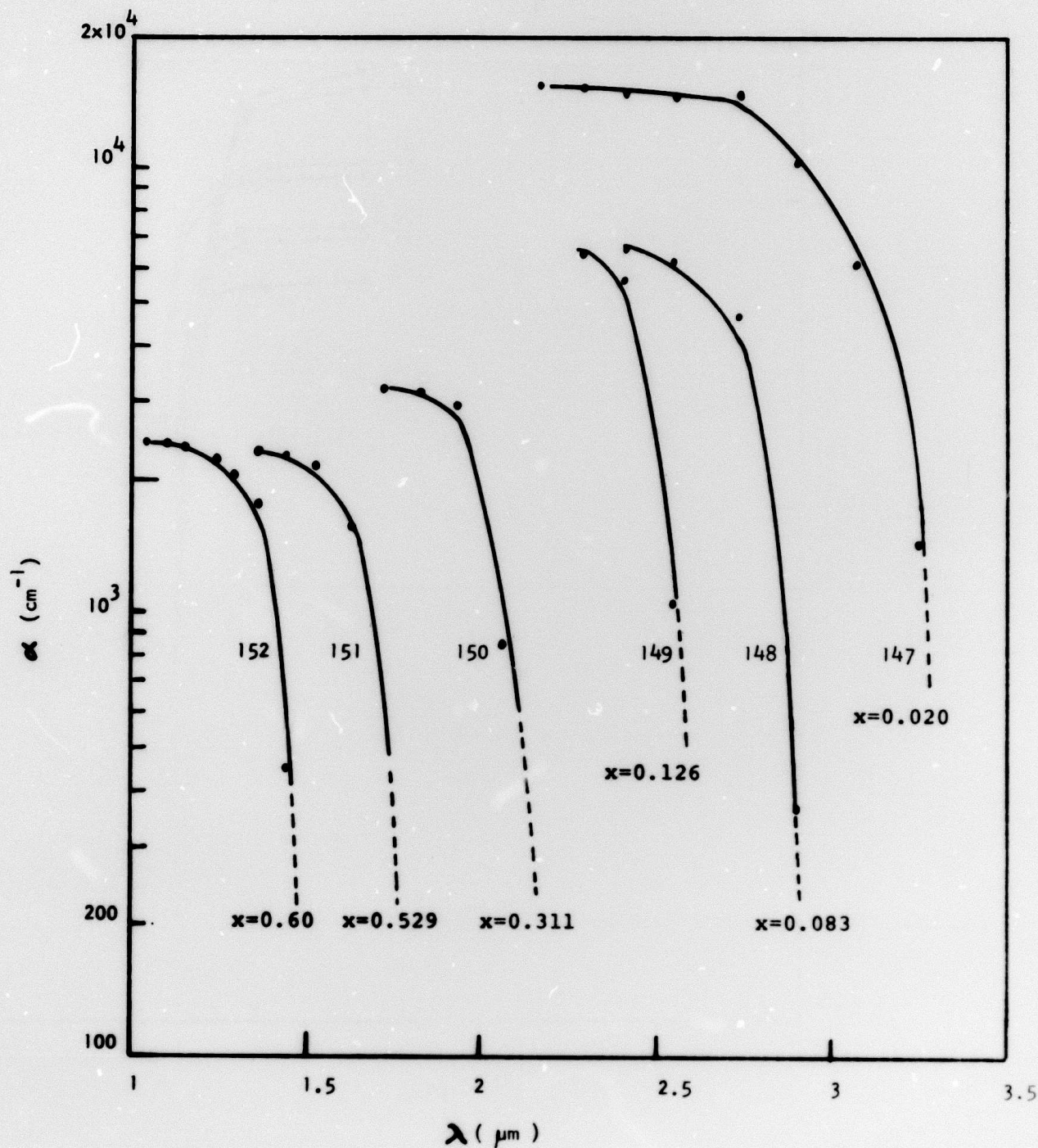


Fig.4.3 The absorption coefficient versus wavelength for six $\text{InAs}_{1-x}\text{P}_x$ epitaxial samples of different alloy compositions

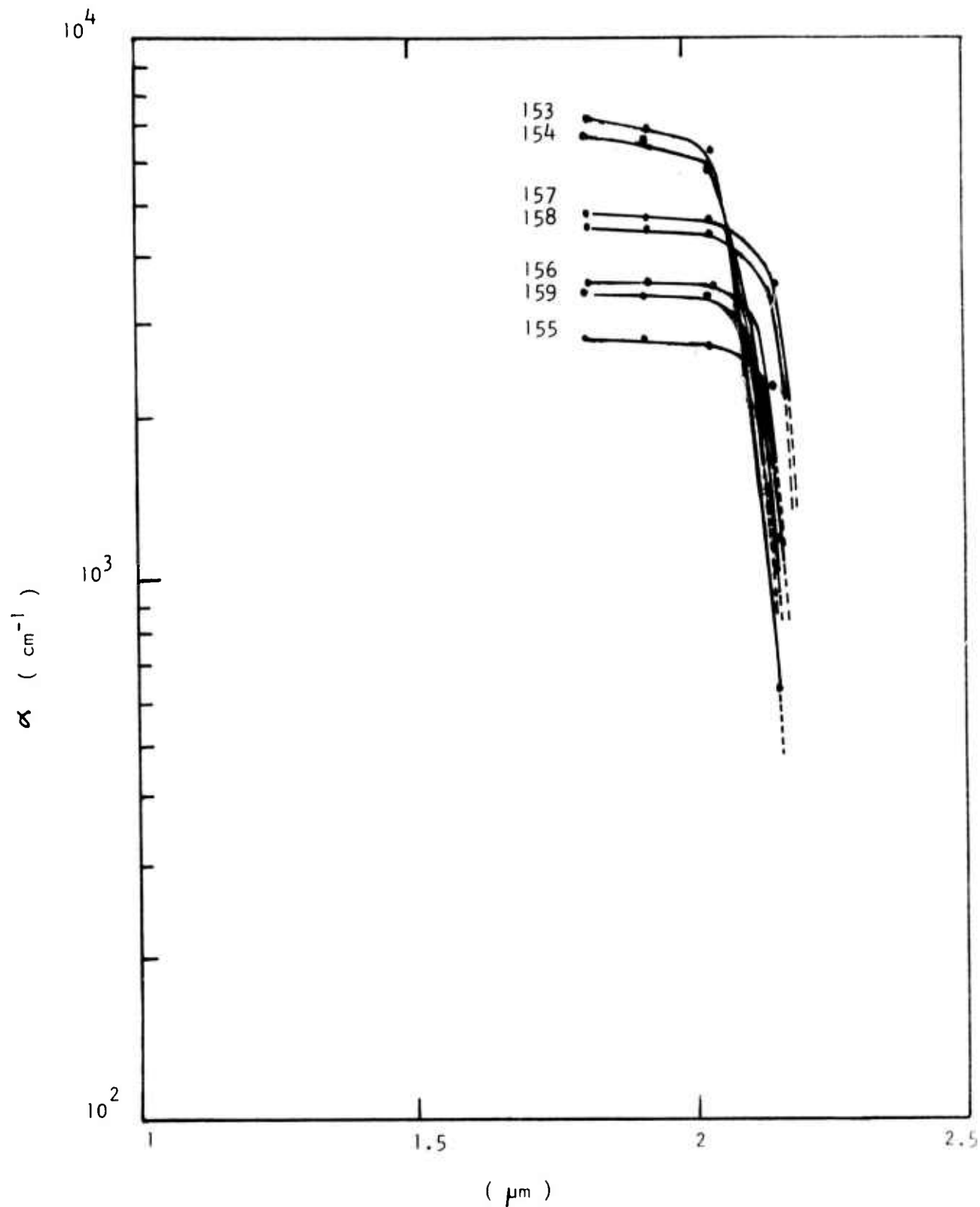


Fig. 4.4 Absorption Coefficient versus Wavelength for seven $\text{InAs}_{0.67}\text{P}_{0.33}$ Epitaxial Samples

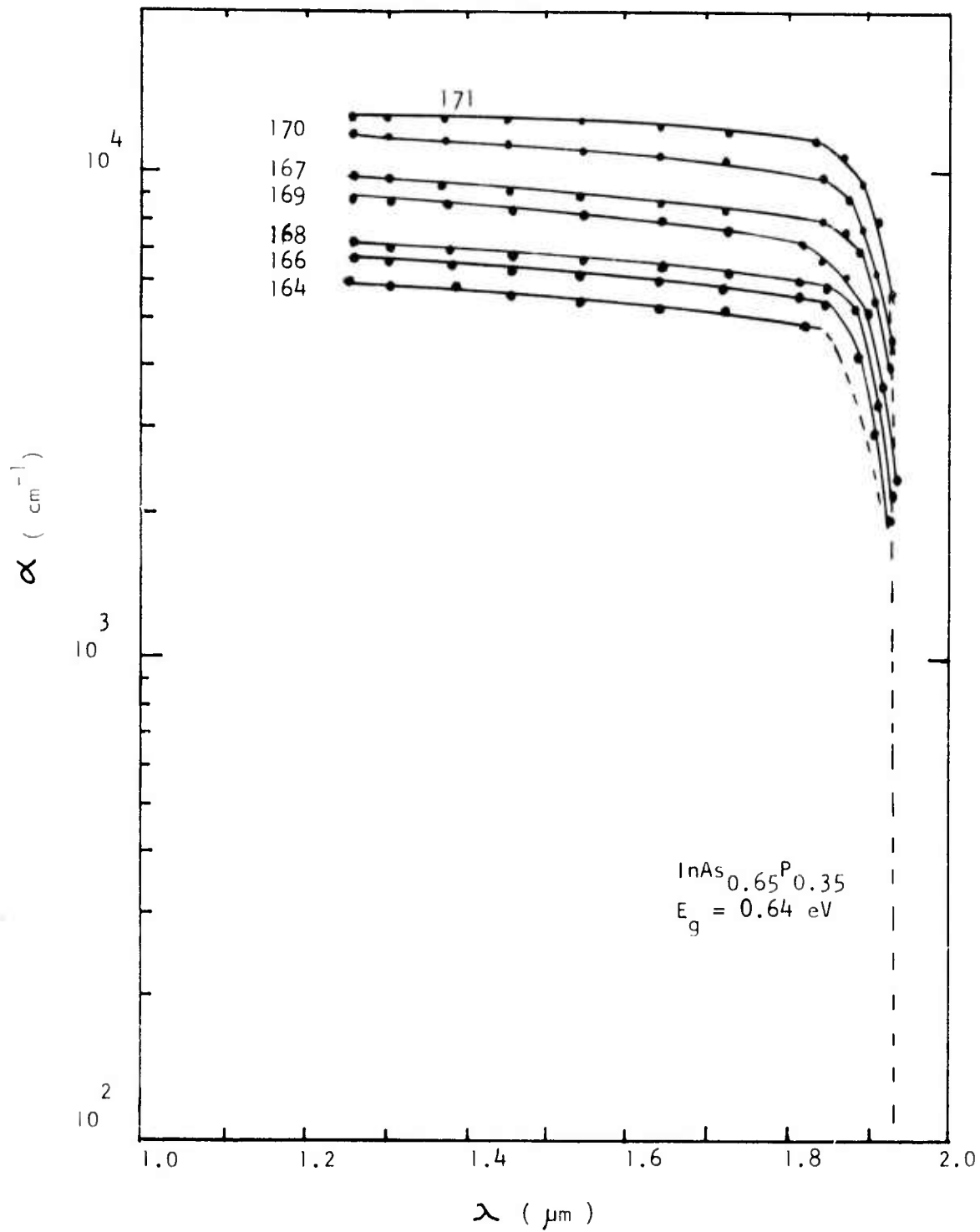


Fig.4.5 Absorption Coefficient versus Wavelength for Seven InAsP Epitaxial Samples with Different H_2 Flow Rates

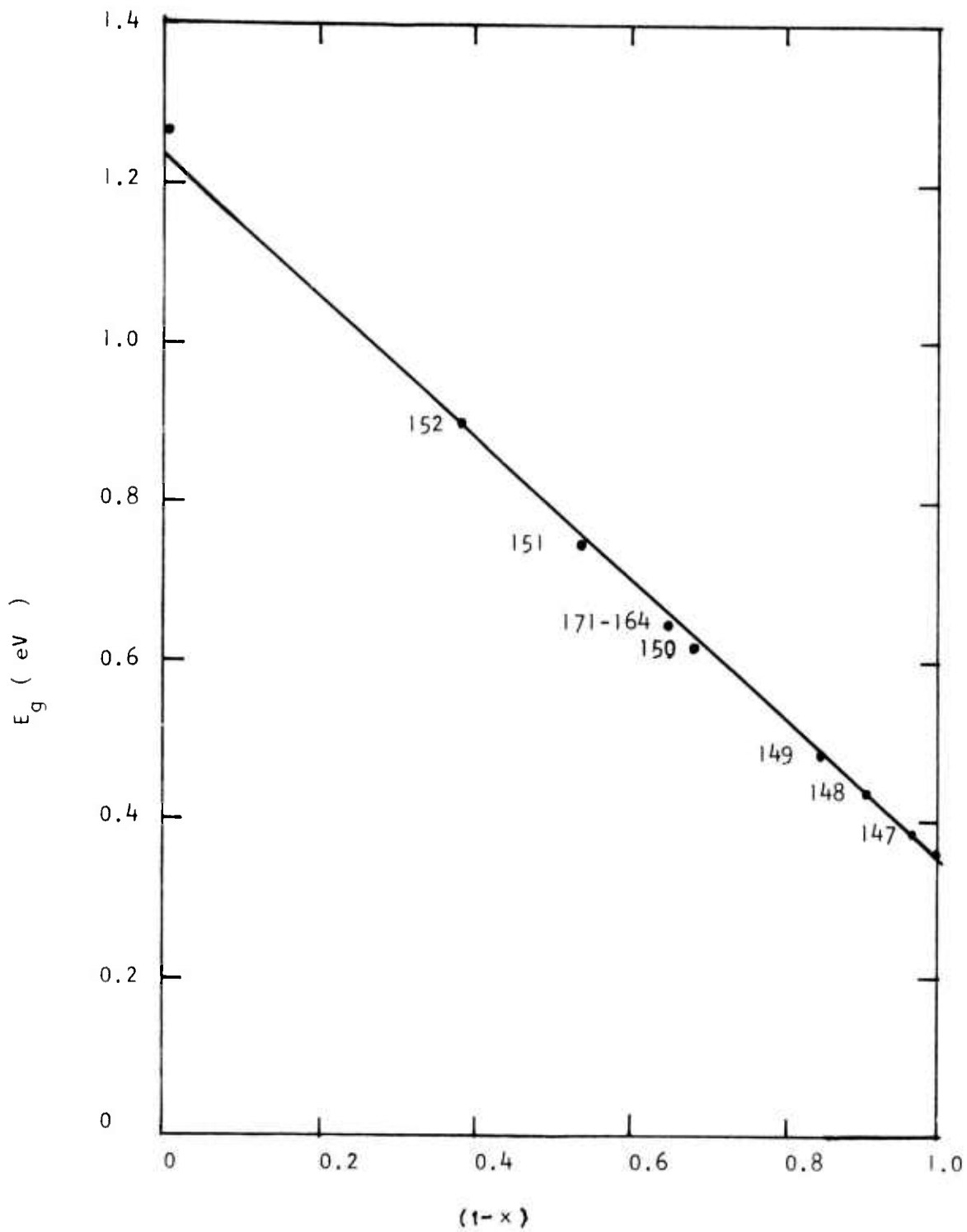


Fig. 4.6 Energy Band Gap versus Alloy Composition for $nAs_{1-x}P_x$ Epitaxial Samples

V. FUTURE PLANS

Results obtained so far yield useful information such as electron mobility and electron concentration for the InAsP epitaxial samples as a function of temperature, the epitaxial layer thickness, and the H₂ flow rate. The optical absorption coefficient as a function of wavelength near the fundamental absorption edge was determined for some bulk and epitaxial InAsP samples of different alloy compositions. Correlations have been obtained between the epilayer thickness and electron mobility and between the thickness and electron concentration for samples of InAs_{0.65}P_{0.35} 164 through 171 (i.e., 10 to 4 μm films).

Our plans for the fifth and sixth quarter of this research contract are (1) to continue our present work with emphasis on the development of a theoretical model to interpret the observed optical and transport parameters in epitaxial InAsP samples; (2) to perform resistivity, Hall effect, reflectance and transmission measurements as well as electron microprobe analysis for epitaxial samples 172 through 178 (which have an epitaxial layer thickness of 2 μm or less); (3) to perform the photoconductivity and the photomagneto-electric effect measurements in the InAsP samples to determine the carrier lifetimes and the impurity states; (4) to study the recombination and scattering mechanisms in this alloy system; and (5) to prepare another set of InAsP epitaxial samples with a fixed epilayer thickness (10 μm) and a different H₂ flow rate.

VI. REFERENCES

1. S. S. Li, "Investigation of Basic Electronic Transport, Recombination and Optical Properties in InAsP Alloy Systems for 1~2 μm IR Applications," First Semi-Annual Technical Report, Contract No. DAAK02-74-C-0102, June 15, 1974.
2. R. K. Willardson and A. C. Beer, "Semiconductors and Semimetals," Vol. 3 Optical Properties of III - V Compounds, Academic Press (1967).